T.C. YEDITEPE UNIVERSITY
INSTITUTE OF HEALTH SCIENCES
DEPARTMENT OF PHARMACEUTICAL TECHNOLOGY

Formulation and Evaluation of Vesicular Carrier Systems Containing Anti alopecia *Serenoa repens* Extract

RIHAM TURKI MOHAMMED BEDR SARAKIBI, MSc

ISTANBUL-2021

T.C. YEDITEPE UNIVERSITY
INSTITUTE OF HEALTH SCIENCES
DEPARTMENT OF PHARMACEUTICAL TECHNOLOGY

Formulation and Evaluation of Vesicular Carrier Systems Containing Anti-alopecia *Serenoa repens* Extract

MASTER THESIS

RIHAM TURKI MOHAMMED BEDR SARAKIBI, MSc

ADVISOR: Assist. Prof. Dr. Muhammed Abdur RAUF

ISTANBUL-2021

THESIS APPROVAL

Institute	:Yeditepe University Institute of Health Sciences
Programme	: Master in Drug and Cosmetics Production Technologies
Title of the Thesis	: Formulation and Evaluation of Vesicular Carrier Systems Containing Anti-alopecia *Serenoa repens* Extract
Owner of the Thesis	: RIHAM TURKI MOHAMMED BEDR SARAKIBI
Examination Date	: 05.07.2021

This study has been approved in content and quality by the Jury as a Master Thesis.

	Title, Name-Surname (Institution)
Chair of the Jury (Advisor):	Assist.Prof.Dr. Muhammed Abdur RAUF, Yeditepe University
Member/Examiner:	Assist.Prof.Dr. Yasemin Uzuner, Acıbadem University
Member/Examiner:	Assist.Prof.Dr. Samet Özdemir, İstanbul Health and Technology University

APPROVAL

This thesis has been deemed appropriate by the above jury in accordance with the relevant articles of Yeditepe University Graduate Education and Examinations Regulation and has been approved by Institute Administrative Board with decision dated ..... and numbered .....

Prof. Dr. Bayram YILMAZ

Director of Institute of Health Sciences

DECLARATION

I hereby declare that this thesis is my own work and that, to the best of my knowledge and belief, it contains no material previously published or written by another person nor material which has been accepted for the award of any other degree except where due acknowledgement has been made in the text.

05.07.2021

Riham Turki Mohammed Bedr Sarakibi

DEDICATION

To my parents, husband, and my dear daughter Perihan …

ACKNOWLEDGMENT

I would like to express my thankfulness to those who supported me to accomplish this study.

First of all, I would like to state my gratitude to my advisor Assist Prof. Dr. Muhammed Abdur Rauf for his support and guidance throughout my study period in the university.

Then, I would like to extend my sincere appreciation to Assist. Prof. Dr. Ebru Turkoz Acar and Prof. Dr. Çetin Taş for sharing their scientific theoretical and practical experiences with me during my research.

Additionally, I'd like to thank the technical specialist Bilal Şenkal and Tuncay Yerli for their continuous help during my research.

Of course, I must convey my thanks to my friends, Rawan Ranna, Ahmed Wadi, and, especially, Najwa Rashad for their substantial and incorporeal support during my study and research.

Finally, my furthermost thanks go to my parents Eman Osman and Dr.Turki Sarakbi who gave priceless lifetime support, to my sister Rowayda, my husband Fayaz, and my brothers Mohammed and Manar for their boundless and unconditional support.

TABLE OF CONTENTS

LIST OF TABLES

LIST OF FIGURES

LIST OF SYMBOLS AND ABBREVIATIONS

µg	Microgram
µm	Micrometer
AGA	Androgenic alopecia
A	Area of membrane subjected to the permeant in cm^2
AI	Active ingredient
C_a	Actual concentration
C_f	Found concentration
Ci	Concentrations of the permeant on the receptor side
cm^{-1}	Per centimeter
CO_2	Carbon dioxide
coeff.	Coefficient
cP	Centipoise
DHT	Dihydrotestosterone
DI	Deformability index
DLS	Dynamic light scattering
EE %	Entrapment efficiency
Eq	Equation
evap. temp.	Evaporation temperature
FDA	Food and drug administration
FF-TEM	Freeze fracture replication-electron microscopy
HPLC	High-performance liquid chromatography,
hr	Hour
IC50	The half-maximal inhibitory concentration
IVRT	In vitro release test
J	Flux
Jss	Steady-state flux
Kp	Permeability constant
L	Liter
LC/ESI-MS	Liquid chromatography-electrospray ionization tandem mass spectrometry
LSESr	Lipido-sterol extract of Saw Palmetto
M	Mole
min	Minute
ML	Methyl laurate
mL	Milliliter
MLnio	Methyl laurate niosome
mM	Millimole

Na-cholate	Sodium cholate
nm	Nanometer
PBS	Phosphated buffer saline
PDI	Polydispersity index
PVT	Performance verification test
Q	Quantity of permeant crossed the membrane
R^2	Fitness coefficient
rpm	Rotation per minute
Sa	The size of vesicles after extrusion
Sb	The size of vesicles before extrusion
SC	Stratum corneum
SEM	Scanning electron microscopy
SHBG	Sex hormone-binding globulin
SPE	Saw palmetto extract
SUPAC-SS	Scale-Up and Post-Approval Changes- Semi-solid
TEM	Transmission electron microscopy
UDN	Ultra deformable niosome
v/v	Volume by volume

ABSTRACT

Sarakibi, RTMB. (2021). Formulation and Evaluation of Vesicular Carrier Systems Containing Anti alopecia *Serenoa repens* Extract. Yeditepe University, Institute of Health Sciences, Drug and Cosmetics Production Technologies, Istanbul. Androgenic Alopecia is primarily caused by dihydrotestosterone, which is mediated by 5-α reductase enzyme. This can be reasonably treated by a 5-α reductase inhibitor. *Serenoa repens*, commonly known as "Saw Palmetto", extract has shown inhibitory activity against 5-α reductase enzyme, which is believed to be due to the presence of many 5-α reductase inhibiting components, mainly, methyl laurate. Methyl laurate (ML) has significant activity against both isotypes of 5α-reductase enzyme. The nature and size of niosomes make them great carriers for these anti-alopecia agents to aid deeper penetration and longer residence in the follicular sink. Niosomes were prepared using Span 60, Tween 60, and cholesterol with the addition of sodium cholate to increase the elasticity of the vesicles by thin-film hydration method. The thin films of these components together with either methyl laureate or Saw Palmetto extract were hydrated by pH 5.5-phosphate buffer saline (PBS). The average size of vesicles was 185 and 176 nm for methyl laurate and the Saw Palmetto (SP) extract vesicles, respectively. Their polydispersity indexes were 0.4 and 0.3, respectively, indicating homogeneity. Zeta potential values for these vesicles were -17.3 and -17.8 mV whereas their deformability indexes were 0.89 and 1.06, respectively. Two mg of ML could be loaded for every 0.1 mM surfactant. These vesicles exhibited acceptable stability over 6-month period. Methyl laureate loaded vesicles were subjected to permeability testing through a skin alternative artificial membrane, Strat-M, and showed significant flux (P= 0.0087), permeability (P=0.0075), and cumulative permeability (P=0.0007). Finally, loaded niosomes were incorporated into carboxymethyl cellulose gel formulation with a final concentration of 0.1 % (w/w). Rheograms of gel formulations showed a plastic behavior. The plastic viscosities of these gels were 9.27-9.44 centiPoise (cP). In conclusion, niosomes are applicable delivery carriers for anti-alopecia agents *Saw Palmetto* extract and its component methyl laurate, and are good candidates for *in vivo* efficacy assessment.

Key Words: androgenic alopecia, niosome, saw palmetto, methyl laurate, gel

ÖZET

Sarakibi, RTMB. (2021). Anti-alopesi *Serenoa repens* Ekstresi içeren Veziküler Taşıyıcı Sistemlerin Formülasyonu ve Değerlendirilmesi. Yeditepe Üniversitesi Sağlık Bilimleri Enstitüsü, İlaç ve Kozmetik Üretim Teknolojileri, İstanbul.

Androjenik alopesi, öncelikle 5-alfa redüktaz enziminin aracılık ettiği dihidrotestosterondan kaynaklanır. Bu, bir 5-alfa redüktaz inhibitörü ile makul bir şekilde tedavi edilebilir. Yaygın olarak "Saw Palmetto" (Cüce Palmiye) özü olarak bilinen *Serenoa repens*, başta metil laurat olmak üzere birçok 5-alfa redüktaz inhibe edici bileşenin varlığından kaynaklandığına inanılan 5-alfa redüktaz enzimine karşı inhibitör aktivite göstermiştir. Metil laurat, 5-alfa-redüktaz enziminin her iki izotipine karşı önemli bir aktiviteye sahiptir. Niozomların doğası ve boyutu, onları bu alopesi önleyici ajanların foliküler havuzda daha derin penetrasyona ve daha uzun süre kalıcılığa yardımcı olması için uygun taşıyıcı yapar. Span 60, Tween 60 ve kolesterol kullanılarak veziküllerin elastikiyetini artırmak için sodyum kolat ilavesiyle ince film hidrasyon yöntemi ile niozomlar hazırlanmıştır. Metil laurat veya Saw Palmetto özütü ile birlikte bu bileşenlerin ince filmleri pH 5.5 fosfat tamponlu tuzlu su (PBS) ile hidratlanmıştır. Veziküllerin ortalama boyutu, metil laurat ve Saw Palmetto (SP) özütü için sırasıyla 185 ve 176 nm idi. Homojenliği gösteren polidispersite indeksleri, sırasıyla 0.4 ve 0.3 idi. Bu veziküller için zeta potansiyel değerleri -17,3 ve -17,8 mV iken deforme olma indeksleri sırasıyla 0,89 ve 1,06 idi. Her 0.1 mM surfaktan iki mg ML'yi yükleme kapasitesini göstermiştir. Bu veziküller 6 aylık bir süre boyunca kabul edilebilir stabilite sergiledi. Metil laurat yüklü veziküller, deriye alternatif bir yapay membran olan Strat-M aracılığıyla geçirgenlik testine tabi tutulmuş ve önemli akı (P= 0.0087), geçirgenlik (P=0.0075) ve kümülatif geçirgenlik (P=0.0007) göstermıştır. Son olarak, yüklenen niozomlar, %0.1 (a/a) nihai konsantrasyonla karboksimetil selüloz jel formülasyonuna dahil edilmiştir. Jel formülasyonların reogramları plastik bir davranış göstermiştir. Bu jellerin plastik viskoziteleri 9.27-9.44 santiPoise (cP) olarak bulunmuştur.. Sonuç olarak, niozomlar, anti-alopesi ajanları Saw Palmetto özütü ve bunun etkili bileşen metil lauratı için uygulanabilir taşıyıcılardır ve in vivo etkinlik değerlendirmesi için iyi adaylardır.

Anahtar Kelimeler: androjenik alopesi, niozom, Saw Palmetto, metil laurat, jel

1. INTRODUCTION AND PURPOSE

Alopecia, a common problem among male and, to some extent, female populations around the world with the most common type being androgenic alopecia (AGA), is mainly caused by dihydrotestosterone which is mediated by 5-α reductase enzyme (1) and micro-inflammation among other factors. Management includes dietary and lifestyle innovations to counteract the complications associated with alopecia (2), in addition to oral and/or topical medications such as oral finasteride, an oral anti-androgen (for women), topical minoxidil, and topical latanoprost (1). However, the activity of the topical treatments present in the market is questionable and not fully satisfying (2). This is due to several side effects and/or poor skin penetration of the anti-alopecia ingredients.

Novel drug delivery systems and carriers such as particulate, polymeric (micelles), molecular and vesicular carriers received significant recognition in the past few decades (3). Vesicular carrier systems, for example, liposomes, transfersomes, ethosomes, niosomes, etc have been proven effective to augment skin penetration of different lipophilic and hydrophilic compounds (4-6).

Niosomes, for instance, are promising lamellar carriers for both hydrophilic and lipophilic substances (7). They can be used for different routes of administration to increase the bioavailability of the drug by enhancing penetration and diffusion through biological membranes (8). Their bilayer structure similar to liposomes makes them ideal for improved transdermal delivery (9), while their submicron size (ranging between 20 and 1000 nm) makes them perfect for hair follicle penetration (10).

Serenoa repens, "Saw Palmetto", extract (SPE) has shown significant inhibitory activity in *in vitro* test against 5-α reductase enzyme (11-15) which is believed to be the main cause for AGA. It has also been shown to have good activity when consumed orally (16). However, the topical activity was not as significant as expected although some activity was shown (17-18). This is probably due to poor skin penetration. The existence of numerous phytosterols involving β-sitosterol, stigmasterol, and campesterol might suggest where the 5α-reductase inhibitory activity of Saw Palmetto originates from (2). Moreover, oleic and lauric acids were isolated upon column and preparative-HPLC analysis of *Saw Palmetto* extract (SPE) and were linked to the pharmacological

activity of the extract. These components exhibit specific binding to the autonomic receptors, involving α1-adrenergic, muscarinic, and 1,4- dihydropyridine receptors. The potency of oleic and lauric acids against 5α-reductase enzyme activity was revealed by LC/ESI-MS-based enzyme experiments (19).

Methyl laurate (ML), one of the most abundant components of SPE, has significant activity against 5-α reductase enzyme. Some studies even attribute the activity of the extract with the existence of lauric acid and/or its methyl esters.

The aim of this study is to formulate and characterize niosomes carrying *Serenoa repens* extract and methyl laurate, study the transfer of the vesicles across a skin equivalent artificial membrane, and incorporate them into gel preparations to enhance their shelf stability and ease of application onto the scalp.

2. LITERATURE REVIEW

2.1. Hair Structure and Anatomy

Hairs are elongated keratinized structures consisting of bulbs and shafts, which are formed within epidermal invaginations of the hair follicles (Figure 2.1). The color, size, shape, and texture of hair differ with age, genetics, and zone of the body. Hairs grow intermittently i.e. with phases of growth followed by phases of rest.

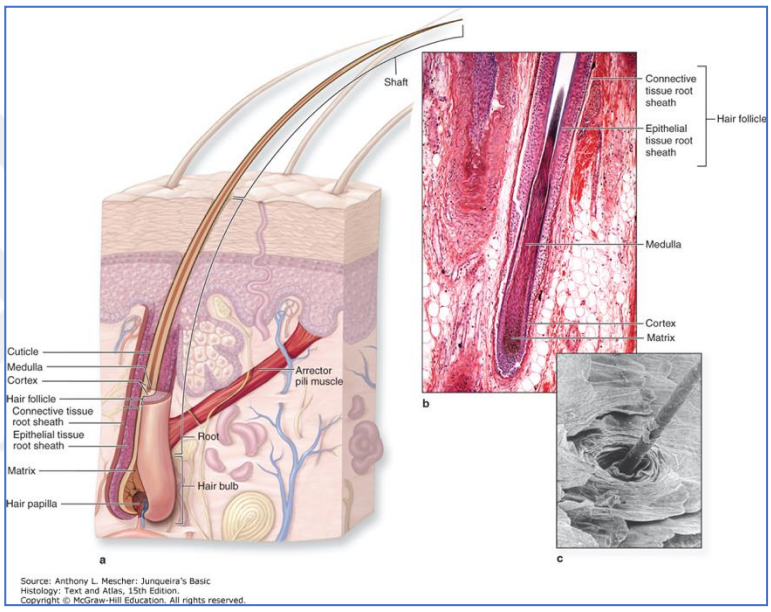

Figure 2.1. Structure of hair follicle (1)

The diagram demonstrates key sections of a hair shaft and hair follicle, showing vascular papilla which is responsible for hair nutrition, and the arrector pili muscle which is responsible for the hair erection. In the growth phase of the hair follicle, it possesses a terminal expansion named a “hair bulb” (20). The dermal papilla implants in the hair bulb and forms a network of capillaries that is needed to maintain the hair follicle. The keratin cells “Keratinocytes” together with the cells of the basal epidermis enclose the dermal papilla and these cells represent the matrix of the elongating hair

root (20). On the other hand, the portion of a hair outspreading away from the skin surface is called the “hair shaft”.

In the matrix region closely around the dermal papilla, the keratinocytes of the hair bulb divide promptly and then undergo keratinization. Also, the terminal differentiation and melanin build up take place at the same site. The hair keratin is firm and more packed than the keratin of the stratum corneum, which maintains its structure while the hair shaft grows further (20).

The hair can be divided into three sections (21-22) lengthwise:

a) A bulge at the base originating from the dermis called the bulb
b) The part of the hair lying underneath the skin surface called the root
c) The hair above the skin surface called the shaft

In cross-section, there are also three parts (21-22):

a) The area in the core containing loose cells and airspaces, called the medulla.
b) A densely, packed keratin, called the cortex.
c) A single layer of cells is arranged like roof boards, called the cuticle (21-22).

2.1.2. Phases of Hair Growth Cycle

As shown in Figure 2.2 a-e

a) A long mitotic phase (anagen): in which the hair matrix has speedily proliferating epithelial cells, and is extremely sensitive to growth factors, drugs, stress, hormones, and immunologic and physical injury.

b) A short phase of hindered growth and deterioration of the hair bulb (catagen): Apoptosis-driven phase between telogen and anagen phase

c) A final long period of inactivity (telogen): a period of relative dormancy prior to shedding in which the hairs have depigmented rounded proximal ends.

d) Exogen Active process of hair shedding

e) the precursor cells for the matrix of a new hair bulb are generated once the next anagen phase begins by epidermal stem cells located in the exterior root sheath adjacent to the arrector pili muscle (1, 20).

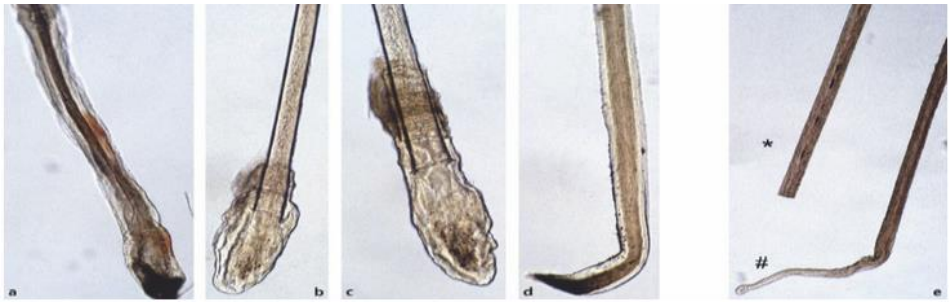

Figure 2.2. Phases of hair growth cycle; a: anagen hair, b: telogen hair; c: catagen hair; d: anagen dysplastic hair, e: #dystrophic hair, * broken hair (21)

2.2. Alopecia

"Effluvium" or "defluvium" is a term that describes hair shedding, and the resultant disorder is named alopecia (Greek alópekia, "baldness") (1).

"Scarring" and "non-scarring" are the two major forms of alopecia. Scarring alopecia is accompanied by inflammation, fibrosis, and damage of hair follicles. A reduction in the number of hair follicles is frequently observed clinically with an apparent smooth scalp. However, in some patients, a biopsy specimen from affected areas must be taken in order to observe the changes. On the other hand, the hair shafts are missing in nonscarring alopecia or reduced in number, but the hair follicles still exist, that is why nonscarring alopecia is reversible (23).

2.2.1. Types and Causes of Alopecia **(Table 2.1)**

I. Nonscarring alopecia

A. Primary cutaneous disorders

- Androgenetic alopecia
- Alopecia areata
- Traumatic alopecia
- Telogen effluvium
- Tinea capitis
- Psoriasiform alopecia, including TNF-α inhibitor-induced (23)

B. Drugs

C. Systemic diseases

- Systemic lupus erythematosus
- Hypothyroidism
- Secondary Deficiencies of protein, biotin, zinc, and perhaps iron
- syphilis
- Hypopituitarism
- Hyperthyroidism (23)

II. Scarring alopecia

A. Primary cutaneous disorders

- Cutaneous lupus (chronic discoid lesions)
- Lichen planus, including frontal fibrosing alopecia
- Central centrifugal cicatricial alopecia
- Folliculitis decal vans
- Linear morphea (linear scleroderma) (23)

B. Systemic diseases

- Discoid lesions in the setting of systemic lupus erythematosus
- Cutaneous metastases
- Sarcoidosis (23)

Alopecia areata, androgenetic alopecia, tinea capitis, telogen effluvium, and the early phase of traumatic alopecia are the most common types of nonscarring alopecia (23).

Table 2.1. Types, causes, characteristics, and suggested treatment of alopecia (23)

	Clinical Characteristics	Pathogenesis	Treatment
Telogen effluvium	Diffuse shedding of normal hairs Follows major stress (high fever, severe infection) or change in hormone levels (postpartum) Reversible without treatment	Stress causes more of the asynchronous growth cycles of individual hairs to become synchronous; therefore, larger numbers of growing (anagen) hairs simultaneously enter the dying (telogen) phase	Observation; discontinue any drugs that have alopecia as a side effect; must exclude underlying metabolic causes, e.g., hypothyroidism, hyperthyroidism
Androgenetic alopecia (male pattern; female pattern)	Miniaturization of hairs along the midline of the scalp Recession of the anterior scalp line in men and some women	Increased sensitivity of affected hairs to the effects of androgens Increased levels of circulating androgens (ovarian or adrenal source in women)	If no evidence of hyperandrogenemia, then topical minoxidil; finasteride[a]; spironolactone (women); hair transplant
Alopecia areata	Well-circumscribed, circular areas of hair loss, 2–5 cm in diameter In extensive cases, coalescence of lesions and/or involvement of other hair-bearing surfaces of the body Pitting or sandpapered appearance of the nails	The germinative zones of the hair follicles are surrounded by T lymphocytes Occasional associated diseases: hyperthyroidism, hypothyroidism, vitiligo, Down syndrome	Topical anthralin or tazarotene; intralesional glucocorticoids; topical contact sensitizers; JAK inhibitors
Tinea capitis	Varies from scaling with minimal hair loss to discrete patches with "black dots" (sites of broken infected hairs) to boggy plaque with pustules (kerion)[b]	Invasion of hairs by dermatophytes, most commonly *Trichophyton tonsurans*	Oral griseofulvin or terbinafine plus 2.5% selenium sulfide or ketoconazole shampoo; examine family members
Traumatic alopecia[c]	Broken hairs, often of varying lengths Irregular outline in trichotillomania and traction alopecia	Traction with curlers, rubber bands, tight braiding Exposure to heat or chemicals (e.g., hair straighteners) Mechanical pulling (trichotillomania)	Discontinuation of offending hair style or chemical treatments; diagnosis of trichotillomania may require observation of shaved hairs (for growth) or biopsy, possibly followed by psychotherapy

2.2.2. Pattern Hair Loss (Androgenetic alopecia AGA)

It is the most common type of progressive balding in men and women. It's classified according to severity and pattern into Hamilton's classification for AGA in men and Ludwig's classification for AGA in women (1) (Figure 2.3. A and B)

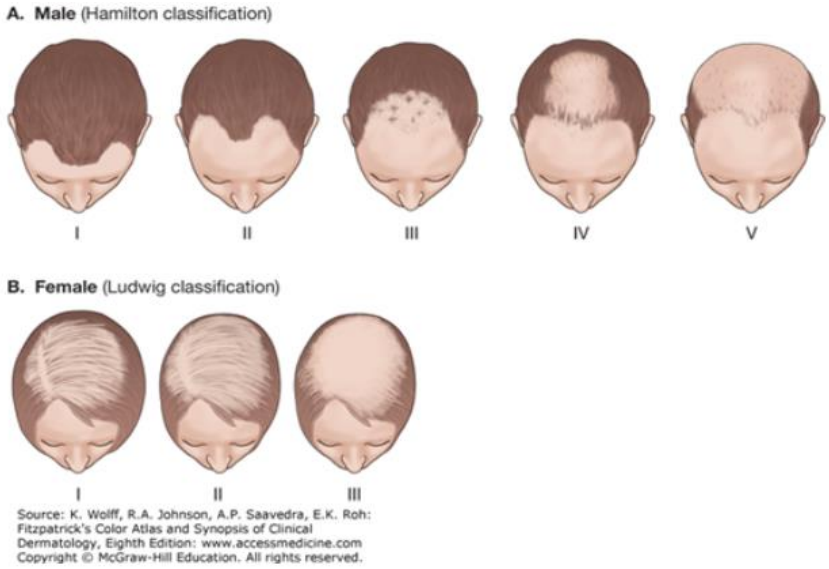

Figure 2.3. Hamilton's classification for (A) AGA in men and Ludwig's classification for (B) AGA in women (1)

Pathogenesis

Primary: Dihydrotestosterone is considered the main pathogenic factor for AGA. Testosterone and Dihydrotestosterone are endogenous androgen sex hormones. Testosterone's function is to promote the growth of the phallus and scrotum, growth of axillary hair and lower pubic hair, spermatogenesis, and sex drive. On the other hand, dihydrotestosterone is responsible for the growth of the prostate, terminal hair, acne, and AGA. Testosterone is converted to dihydrotestosterone by an enzyme called "5α-reductase", from which two isozymes are present: type I and type II. Type I 5α-reductase is located in sebaceous glands found in the scalp, face, chest, and back skin, as well as in the adrenal gland, liver, and kidney. While type II 5α-reductase is localized in the hair follicles of the scalp, beard, and chest, as well as liver, seminal vesicle, prostate, epididymis, and scrotum (1).

Secondary:

Insulin resistance: is interrelated with AGA since the majority of serum androgens frequently bind to sex hormone binding globulins (SHBGs) (2). However, a "high free androgen index" where the relative amount of free androgens to bound androgens is high both in AGA and insulin resistance, therefore, low SHBG levels arise

in both disorders (2). Although it is not fully understood how this is engaged in AGA pathogenesis, it is clearly understood that the complex created with both SHBG and its respective androgen performs a biological function that cannot be carried out by the free androgen (2).

Micro-inflammation: The expression 'microinflammation' was devised by researchers, who theorized that it progressively precedes to a fibroplasia of the dermal sheath encircling the hair follicle, which leads to coiling and shrinking of the pilosebaceous unit. this process is gradual, tacit, and painless progress, but is yet an inflammatory state that finally contributes to the etiology of AGA (2).

Cicatricial alopecia: hair shedding in common cases of AGA can be aggravated by the usage of certain damaging topical substances like inadequately formulated hair oils which nurture lipophilic bacteria which in turn increases microbial growth and inflammation, leading to a fibrosing type of alopecia (2).

Management

Oral: Finasteride (1 mg) is one of the most common oral treatments of AGA. Having no affinity to bind with androgen receptors, Finasteride does not prevent other activities of testosterone such as spermatogenesis, growth of the phallus and scrotum, or libido. However, 2% of men consuming finasteride report decreased libido and erectile dysfunction. On the other hand, Dutasteride (2.5 mg) inhibits both types I and II reductase enzymes, possibly more effectively than finasteride, but at the same time, it has shown the same side effect with more severity.

Topical: Minoxidil is the most widespread topical treatment for AGA and other types of alopecia. Topical minoxidil, 2% and 5% solution are perhaps useful in decreasing the speed of hair loss or somewhat in restoring missing hair in both women and men, however, it causes side effects including irritation, redness, and itching, in addition to tachycardia, chest pain and dizziness if it is absorbed into the circulation. Latanoprost 0.1% is another topical treatment for AGA. It is a prostaglandin analog, which may promote hair follicle growth.

Antiandrogens: spironolactone, cyproterone acetate, flutamide, and cimetidine are particularly used for women suffering from AGA while having high adrenal androgens. They block the action of DHT thru binding to androgen receptors. These are contraindicated for men (1, 24-25).

Other treatment options: including the laser comb, a device lately accepted in the United States for managing male and female pattern alopecia. Moreover, Hair transplantation is a choice for patients with stable AGA (26).

In most cases, AGA is caused by a mishmash of etiologies; thus, one treatment improving just one of these pathologies will hold a minor enhancement in alopecia or a decelerating of the progression. Therefore, the best treatment for AGA would employ a series of lifestyle and dietary interventions to attain prohibition of 5α- reductase or cut of DHT, reverse the insulin resistance, elevating of SHBG (sex hormone binding globulin) levels, prevent of the over-colonization by epidermal flora and Demodex mites, treating inflammated scalp and improvement of dietary deficiencies (2).

2.3. Saw Palmetto (*Serenoa repens*) Extract

It is the extract of the berries of the palm tree *Saw Palmetto* (Figure 2.4) which belongs to the Palm family (Arecaceae), distributed in the Southeastern United States counting Florida, Mississippi, Georgia, South Carolina, and Louisiana.

Figure 2.4. Saw Palmetto plant (27-28)

2.3.1. Components

The purified *Saw Palmetto* extract holds 85-90% fatty acids and sterols, besides plenty of tannin, lipases, carotenoids, and sugars (29). Fatty acids include laurate, myristate, palmitate, stearate, oleate, and linoleate; phytosterols include campesterol, stigmasterol, and β-sitosterol. Liquid saw palmetto supplements consist of significant ($p < 0.05$) concentrations of individual and total fatty acids (908.5 mg/g), and phytosterols (2.04 mg/g). The composition is shown in Table 2.2-2.3.

Table 2.2. Fatty acid composition of some Saw Palmetto supplements (30)

Table 2. Fatty acid quantities (mg/g) and composition (% of total fatty acids) in SRM, liquid, and powder saw palmetto supplements.

Supplement	Laurate (C12:0)		Myristate (C14:0)		Palmitate (C16:0)		Stearate (C18:0)		Oleate (C18:1)		Linoleate (C18:2)		Total Fatty Acid	
	mg/g	%	mg/g	%	mg/g	%	mg/g	%	mg/g	%	mg/g	%	mg/g	% *
Liquid Extracts ($n = 7$)														
Doctor's Best	276.6	29.4	105.4	11.2	86.9	9.2	17.5	1.9	313.9	33.4	43.6	4.6	941.3	94.1
GNC Herbal Plus	82.9	8.9	33.8	3.6	94.0	10.1	25.4	2.7	582.3	62.4	59.1	6.3	933.8	93.4
Spring Valley Natural Foods	170.3	18.5	67.6	7.3	85.8	9.3	24.1	2.6	448.5	48.6	53.9	5.8	923.4	92.3
Now Foods	141.6	15.5	51.6	5.7	107.0	11.7	21.1	2.3	438.1	47.9	81.0	8.9	914.7	91.5
Solaray	141.9	15.6	57.1	6.3	90.9	10.0	21.2	2.3	476.0	52.1	55.6	6.1	913.0	91.3
Saw Palmetto Harvesting Company	254.9	28.3	98.5	11.0	84.4	9.4	16.2	1.8	312.5	34.7	34.1	3.8	900.0	90.0
Jarrow Formulas	127.2	15.3	47.5	5.7	93.1	11.2	32.5	3.9	230.2	27.6	248.2	29.8	833.4	83.3
Mean	**170.8** [a]	**18.8** [a]	**65.9** [a]	**7.2** [a]	**91.7** [a]	**10.1** [a]	**22.6** [a]	**2.5** [a]	**400.2** [a]	**43.8** [a]	**82.2** [a]	**9.3** [a]	**908.5** [a]	**90.9** [a]
SEM	**18.0**	**1.9**	**6.9**	**0.7**	**2.0**	**0.2**	**1.4**	**0.2**	**30.9**	**3.2**	**19.2**	**2.4**	**9.6**	**1.0**
Powders ($n = 5$)														
Permixon	96.7	29.5	38.5	11.8	30.5	9.3	5.6	1.7	111.7	34.1	11.5	3.5	327.3	32.7
Biochem	40.7	17.1	16.2	6.8	58.2	24.4	47.0	19.7	36.4	15.3	19.1	8.0	238.3	23.8
Natures' Way	38.0	26.5	14.3	10.0	18.2	12.7	14.4	10.0	40.1	27.9	6.5	4.5	143.6	14.4
Solaray	40.5	33.7	14.8	12.3	11.9	9.9	2.5	2.1	34.2	28.5	6.1	5.1	120.1	12.0
GNC Saw Palmetto Formula	14.6	21.3	5.6	8.2	15.2	22.1	9.6	13.9	14.6	21.2	4.6	6.7	68.6	6.9
Mean	**46.1** [b]	**25.6** [b]	**17.9** [b]	**9.8** [b]	**26.8** [b]	**15.7** [b]	**15.8** [b]	**9.5** [b]	**47.4** [b]	**25.4** [b]	**9.6** [b]	**5.6** [a]	**179.6** [b]	**18.0** [b]
SEM	**9.0**	**2.0**	**3.7**	**0.7**	**5.7**	**2.1**	**5.4**	**2.3**	**11.1**	**2.2**	**1.8**	**0.5**	**30.7**	**3.1**
Standard Reference Material														
SRM 3251	259.9	26.3	10.6	10.6	86.6	8.5	16.9	1.7	331.1	34.6	50.2	6.0	983.6	98.4

* % of dry mass (weight/weight), different letters indicate significant differences ($p < 0.05$) between the four supplement categories in Tables 2 and 3. Samples and SRM from the same lot, were extracted and analyzed in duplicate.

Table 2.3. Phytosterol composition of some Saw Palmetto supplements (30)

Supplement	Campesterol		Stigmasterol		β-sitosterol		Total Phytosterols	
	mg/g	%	mg/g	%	mg/g	%	mg/g	% *
Liquids								
Jarrow Formulas **	8.33	29.09	4.01	14.03	16.29	56.88	28.63	2.86
Doctor's Best	0.54	19.21	0.24	8.53	2.04	72.26	2.83	0.28
Now Foods	0.29	12.56	0.13	5.66	1.92	81.78	2.35	0.23
Saw Palmetto Harvesting Company	0.34	21.05	0.16	10.09	1.12	68.86	1.62	0.16
Solaray	0.23	11.10	0.11	5.19	1.73	83.71	2.07	0.21
Spring Valley Natural Foods	0.15	7.20	0.11	5.52	1.80	87.28	2.06	0.21
GNC Herbal Plus	0.15	11.61	0.07	5.40	1.08	82.99	1.31	0.13
Mean	0.28 [a]	13.79 [a]	0.14 [a]	6.73 [a]	1.62 [a]	79.48 [a]	2.04 [a]	0.20 [a]
SEM	0.04	1.45	0.02	0.57	0.12	1.99	0.15	0.02
Powders								
Biochem **	22.80	30.30	19.75	26.55	32.55	43.15	75.11	7.51
Permixon	0.18	21.06	0.06	7.68	0.60	71.27	0.84	0.08
Nature's Way	0.10	24.65	0.04	11.11	0.25	64.24	0.39	0.04
Solaray	0.07	23.89	0.03	9.30	0.20	66.80	0.30	0.03
GNC Saw Palmetto Formula	0.03	19.83	0.01	9.19	0.10	70.98	0.15	0.01
Mean	0.09 [b]	22.36 [b]	0.04 [b,c]	9.32 [a]	0.29 [b]	68.32 [b]	0.42 [b]	0.04 [b]
SEM	0.02	0.90	0.01	0.53	0.07	1.33	0.10	0.01
Standard Reference Material								
SRM 3251	0.41	19.69	0.18	8.57	1.48	71.74	2.06	0.21

* % dry mass (weight/weight), ** Jarrow Formulas and Biochem were excluded from statistical analysis due to their very high phytosterol content compared with other supplements. Different letters indicate significant differences ($p < 0.05$) between the four supplement categories in Tables 4 and 5. Samples, and SRM from the same lot, were extracted and analyzed in duplicate.

The Saw Palmetto extract which has been used in this study contains high concentrations of Methyl Laurate, Methyl Oleate, and Trimethylsilyl derivative of sitosterol as shown in the chromatography (Figure 2.5-2.6).

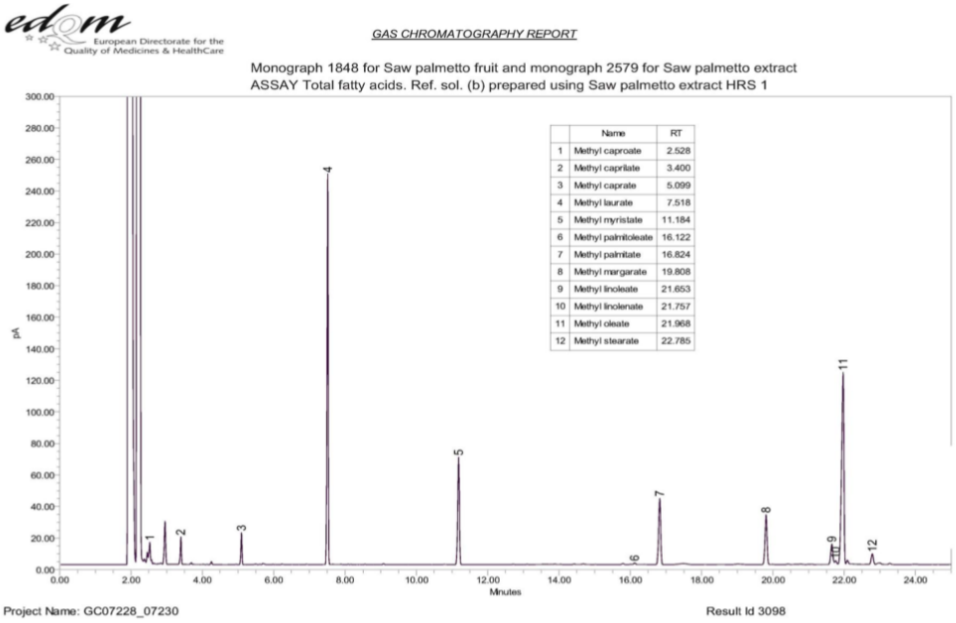

Figure 2.5. Fatty acid components of SPE (31)

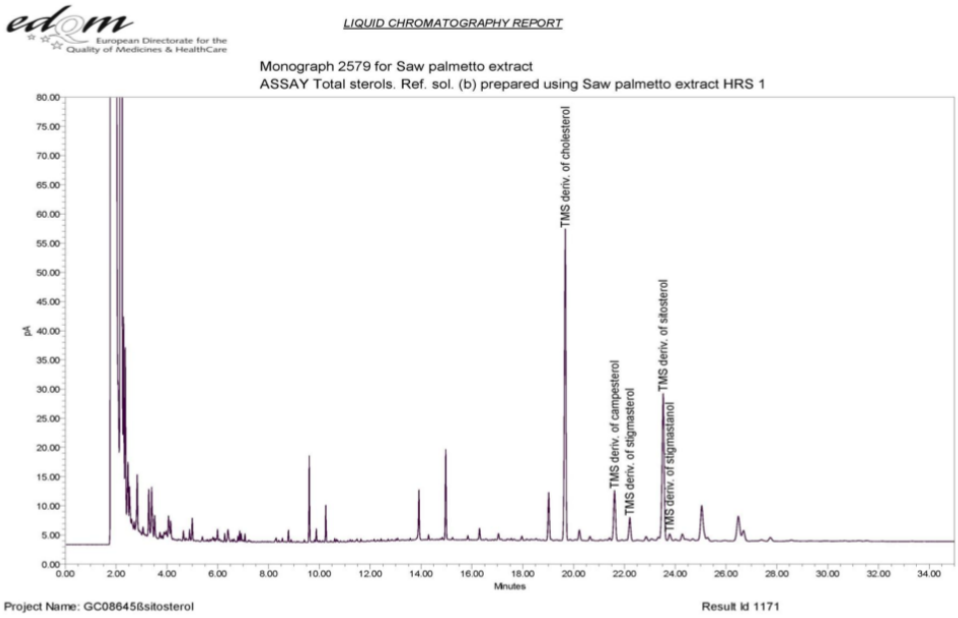

Figure 2.6. Phytosterol components of SPE (31)

2.3.2. Uses

The foremost use of oral Saw Palmetto extract is the management of Benign Prostatic Hyperplasia and the urinary symptoms associated with it (32-33).

It has also been reported, in test-tube tests, to support prostate health and improve prostate cancer (34-35).

Additionally, it has been recounted to be effective in the management of AGA topically and orally (16, 29).

2.3.3. Mechanism of Action and Evidence of Activity against AGA

Saw Palmetto extract is active against AGA through its effect on the main pathogenic factor in AGA: Dihydrotestosterone. It functions by inhibiting 5α-reduction of Testosterone, 3α-reduction of DHT, besides inhibiting DHT from binding to its receptor (11).

In vitro

In one study (Figure 2.7), the inhibition of 5α-reductase both type I and type II by lipido-sterol extract of Saw Palmetto was uncompetitive. It inhibited both isoforms with nearly similar IC_{50} (4 mg/mL for type 1 and 7 mg/mL for type 2) (12).

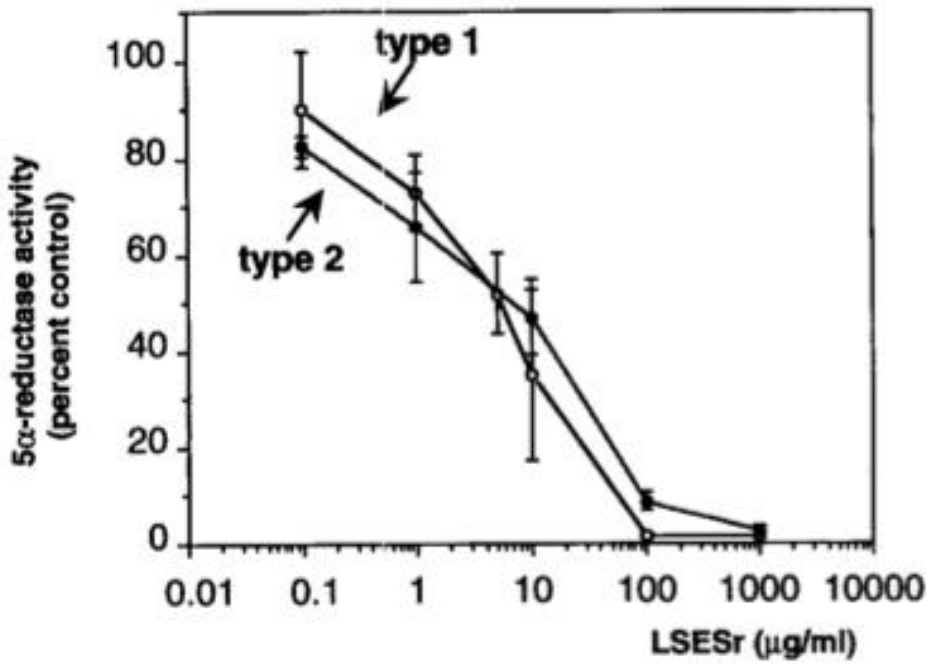

Figure 2.7. The activity of LSESr against 5α-reductase type 1 and 2 (12)

In another in vitro study, n-hexane lipido/sterolic extract of *Saw Palmetto* (10 μg/mL) significantly hindered the activities of both isoenzymes ($p < 0.05$) to a comparable extent (5α-reductase I: 72% decrease; 5α-reductase I: 76% decrease). Though finasteride (5 mM) exhibited a comparable inhibitory effect on 5α-reductase II (83% reduction) in comparison with *Saw Palmetto*, it had no effect on the 5α-reductase I at the same concentration (13).

Another Saw Palmetto supercritical CO_2 extract, concentration-dependently hindered 5α-reductase type II with an IC50 value of 3.58±0.05 μg/mL in vitro (14).

One more Saw Palmetto ethanolic extract was examined in vitro for the blockage capability towards 5α-reductase type II at the concentrations 10, 5, 2.5, 1.25,

1, and 0.5 µg/mL and was found to be a powerful restraint of 5α-reductase type II with an IC_{50} of 2.88±0.45 µg/mL (15).

Lastly, *Saw Palmetto* lipidic extract was shown to inhibit 5α-reductase, 3-ketosteroid reductase besides receptor binding of androgens in cultured human foreskin fibroblasts. A concentration of 28.6 U/mL of the extract drastically modifies the development of Dihydrotestosterone and powerfully inhibits 3-ketosteroid reductase intermediated conversion of Dihydrotestosterone to Sa-androstane-3a, 17fi-diol, while 7.1 U/mL of the extract gives 50% inhibition of the binding of Dihydrotestosterone to its receptor (11).

In vivo

Saw Palmetto extract was estimated effective and safe for the topical treatment of AGA. In one study, the total hair count was boosted by 11.9% in comparison with the pre-treatment period. The concluding ratio of anagen/telogen hair was increased by 38% in comparison with the initials. Concurring to the assessment of vertex photographs, it was confirmed that improvement was notable in 48% of the patients (17).

In another pilot study on 49 patients, the increased hair count was significant at the 12th and 24th week paralleled to the baseline (Figure 2.8.) (18).

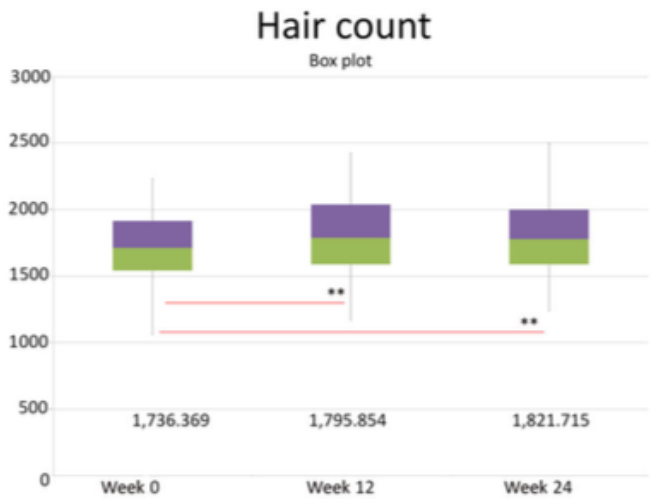

Figure 2.8. Box-whisker plot of average hair count after 12 and 24 weeks of using Saw Palmetto topically (18)

A further pilot study on 26 male subjects ages 23 to 64 with AGA showed a highly positive response to treatment with oral liposterolic extract of *Serenoa repens* (LSESr) and beta-sitosterol. The blinded inspective staff assessment report disclosed that 60% of (6/10) study subjects were regarded as improved at the final visit (16).

The existence of numerous phytosterols including β-sitosterol (6), stigmasterol, and campesterol can suggest wherefrom the 5α-reductase inhibitory efficiency of Saw Palmetto arises (2). Moreover, the column and HPLC separations of the extract documented the presence of oleic and lauric acids as pharmacological active constituents, these components showed an ability to bind to autonomic receptors, counting α1-adrenergic, muscarinic, and Dihydropyridine receptors. At the same time, LC/ESI-MS-based enzyme investigations disclosed the effective hindrance of lauric and oleic acids on 5α-reductase enzyme activity (19).

2.3.4. Methyl Laurate as a Component of Saw Palmetto Extract

Methyl laurate is present in remarkably high concentration in Saw Palmetto extract (31). It was shown to comprise as high as 26.3% up to 30% of some Saw Palmetto extracts (30,36).

It has shown a significant activity against 5α-reductase enzyme with IC50 as low as 17-20 µg/mL in some (lipido-sterolic) Saw Palmetto extracts (36)

And as low as 66.2 µg/mL in some other (supercritical CO_2) Saw Palmetto extracts (19).

These studies suggested that the 5α-reductase inhibitory activity of Saw Palmetto extract is attributable to the presence of Lauric Acid and its Ester.

Methyl laurate is the utmost abundant fatty acid methyl ester present in the SPE used in this study as previously shown in section 2.3.1 the gas chromatography analysis provided in the disclosed leaflet of the extract. Therefore, it was selected as a representative of the extract in some tests for the ease of analysis.

2.4. Niosomes

During the past few decades, extensive concern has been devoted to developing novel systems for drug delivery. Numerous categories of pharmaceutical carriers such as particulate, polymeric, macromolecular and cellular were developed. Particulate type carriers, also identified as colloidal carriers, involves lipid particles, microspheres, and nanoparticles. Polymeric micelles represent the polymeric type carriers, and models of vesicular carriers include liposomes, sphingosome, niosomes, transferosomes, pharmacosomes, virosomes (3, 37).

Some of the Vesicular drug delivery system advantages' are:

1. Extend the systemic subsistence of the drug in circulation.
2. If selective uptake can be succeeded, they can reduce the toxicity of a drug by delivering it directly to its site of action.
3. Enhances the bioavailability particularly of poorly soluble drugs.
4. Suitable for both lipophilic and hydrophilic drugs.
5. Effective for prolonged release of a drug due to its ability to delay the elimination of rapidly metabolized drugs (3).

2.4.1. Definition

Niosomes are lamellar non-ionic surfactant vesicles that are microscopic in size, obtained by hydration of synthetic nonionic surfactants with or without inclusion of cholesterol or other lipids. They can be employed to carry hydrophilic and lipophilic drugs. They are promising carriers for drug delivery and because of their non-ionic nature; they are less toxic and enhance the therapeutic index of drugs through limiting their actions to the target cells. Thus, they are widely used recently as alternatives to liposomes (8-7).

The earliest niosome preparations were modeled and patented by L'Oreal in 1975. Niosomes were first employed in drug delivery for anticancer drugs (9).

2.4.2. Advantages

1. They increase the drug's therapeutic performance via belated clearance from the circulation, which protects the drug from biological environment and limits its validity to target cells.

2. The used surfactants require no special handling or storage.

3. They improve skin penetration of drugs and oral bioavailability of poorly absorbed drugs.

4. They are efficiently formulated to attain the site of the required action by topical, oral, and parenteral routes.

5. They have a substructure involving hydrophilic, amphiphilic and lipophilic moieties at once, and therefore can carry drug molecules with different solubilities (38).

6. They possess great stability, less purity inconsistency, and low cost (39).

7. Simplicity of production in laboratory, and possibility of large scale production (40).

8. Biocompatible, biodegradable, non-immunogenic, and structurally flexible.

9. They can incorporate both water soluble drugs and lipophilic drugs, and are able to extend the circulation of the captured drug in the body (9).

Niosomes have exceptional advantages over liposomes:

1) They are physically and chemically more stable even in the emulsified form.

2) Presence of cholesterol in niosomes increases their hydrodynamic diameter and entrapment efficiency

3) They do not require special protection or storage conditions like low temperature or inert atmosphere.

4) Comparatively reduced cost of materials, making it more fitting for large scale manufacture.

5) They are osmotically active and stable on their own.

6) They increase the stability of the incorporated drugs

7) They exhibit more flexible structure characteristics like size, fluidity, and composition, and they can be designed concurring to the anticipated use.

8) Finally, they are more capable of improving the drug performance by: suspending the drug clearance from the circulation, better targeting the specific site of action, and preserving the drug from biological factors (3).

2.4.3. Structure and Composition of Niosomes

The schematic structure of niosomes are shown in Figure 2.9 below.

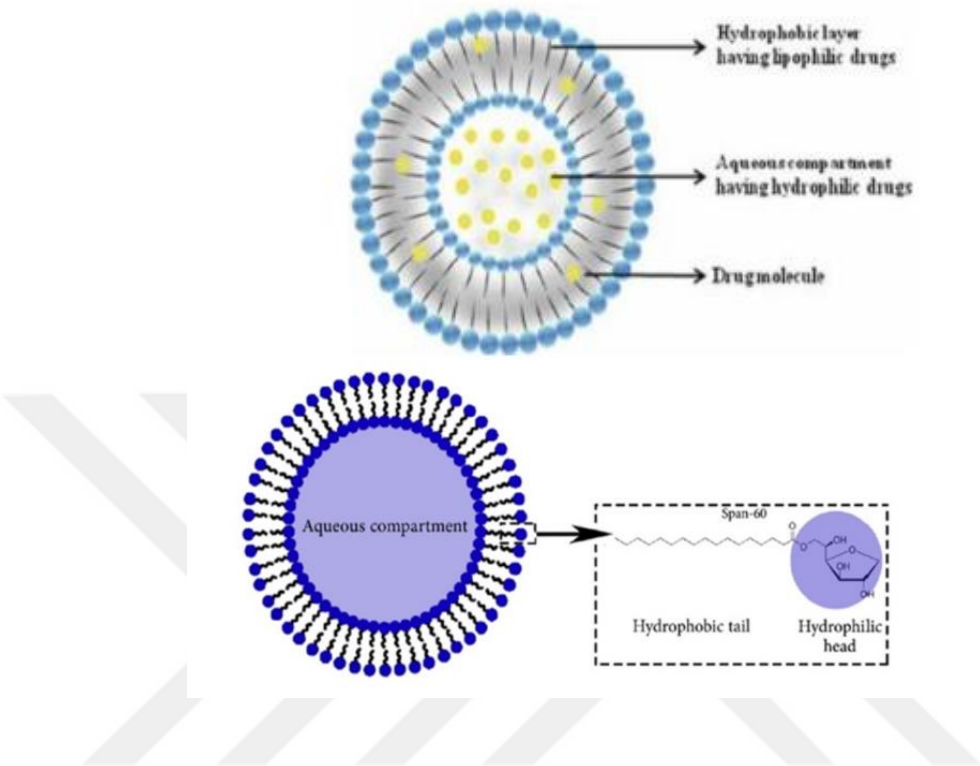

Figure 2.9. Structure and Composition of Niosomes (9, 41-42)

The major ingredients used for formulating niosomes are:

a) Nonionic surfactants: The surfactants playact a major function in the formulation of niosomes. The non-ionic surfactants mentioned below are commonly used to prepare niosomes (9):

1. Spans (span 60, 40, 20, 85, 80)
2. Tweens (tween 20, 40, 60,80).
3. Brijs (brij 30, 35, 52, 58, 72, 76).

b) Cholesterol (Figure 2.10.): employed to provide stiffness, shape, and conformation to the vesicles (9) and reduces drug leakage from niosome (3).

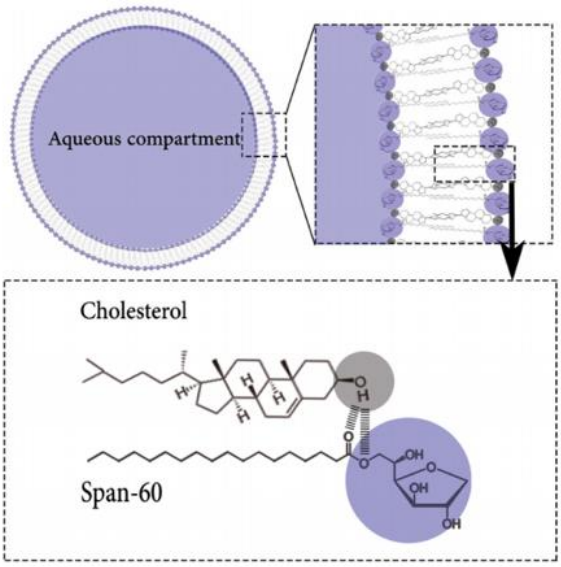

Figure 2.10. Cholesterol insertion in a niosome bilayer (42)

c) Edge activator: they are substance which increase the elasticity of niosome and enhance penetration by providing the maximum deformability of the vesicles (43) such as oleic acid, terpenes (44-45), labrasol, cineole, transcutol, diethylene glycol, and monoethyl ether (46-47).

Other single chain surfactant, exhibiting a high radius of curvature, are able destabilize lipid bilayers to increase their deformability such as Sodium cholate, different Spans and Tweens, and potassium glycyrrhizinate (43, 48-49).

Other materials can be added such as Dicetyl phosphate which is well-known to increase the size, provide charge, and increase the entrapment efficiency, and diacylglycerol that aid in electrostatic stabilization of the vesicles (3).

2.4.4. Mechanism of Skin Permeation

Niosomes increase the rate of transdermal penetration (3), they have higher capability to penetrate the skin than the earlier emulsion preparations due to their structural alikeness to liposomes in owning a bilayer, yet, the ingredients used in preparing niosomes grant further stability and therefore niosomes suggest many more advantages compared to liposomes (9).

2.4.5. Hair Follicle Penetration

The so-called **f**ollicular sink (Figure 2.11), may offer a long-term reservoir for substances and particles applied topically. Targeting the follicular orifices may introduction new routes of drug delivery, though not all hair follicle orifices seem to act as a pool for nanoparticles applied topically because both open and closed follicle orifices are present (50), hair follicle orifices are indeed open throughout sebum production (10, 51) caused by increased levels of DHT (52) which is closely related with androgenic alopecia (1).

The susceptibility of particles of various sizes (600 to 2,500 nm) to accumulate within the orifice of hair follicles was investigated on excised human skin. The particles at a size of 600 nm were found to have the greatest tendency for follicular storage (53).

The penetration of particles with or without massage appeared to be extremely efficient whenever the applied particles were in the same size ordinance as the cuticles of human hair (400 to 700 nm) (54).

Moreover, the particles found within the stratum corneum were noticed to be quantitatively abolished after one day, while particles inside the hair follicles persisted for over 10 days (10, 55)

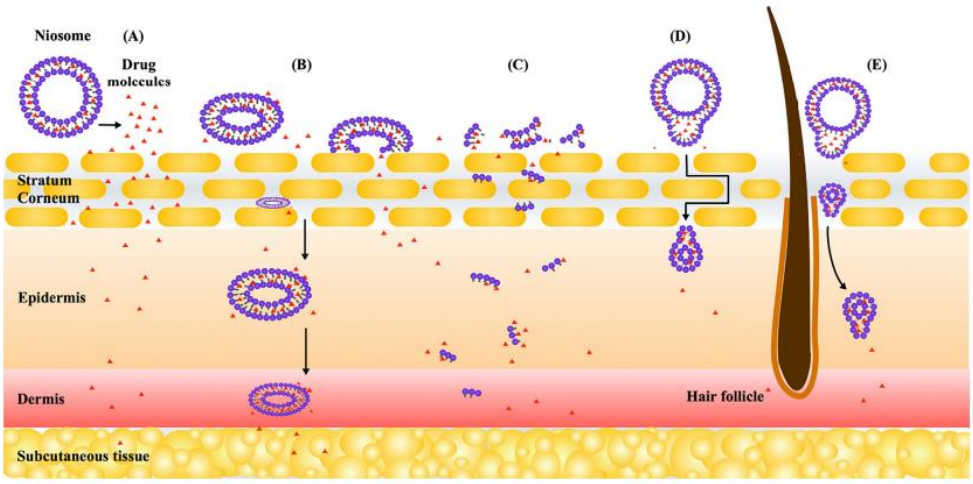

Figure 2.11. Possible mechanisms of niosome dermal and transdermal drug delivery, (A) drug molecules released by niosome; (B) adsorption of niosome and fusion with the SC; (C) niosome pieces penetration through intact SC; (D) elastic niosome with penetration enhancers; (E) niosome penetration through hair follicles (56).

2.4.6. Classification of Niosomes:

Niosomes can be divided into different categories according to their size (Figure 2.12.) (41-42, 57-58):

- Small vesicles, or SV (20-50 nm in diameter),
- Large vesicles, or LV (50-1000 nm in diameter),
- Giant vesicles, or GV (1-20 μm in diameter).

According to the number of membrane bilayers:

- Unilamellar
- Multilamellar
- Oligolamellar
- Multishell

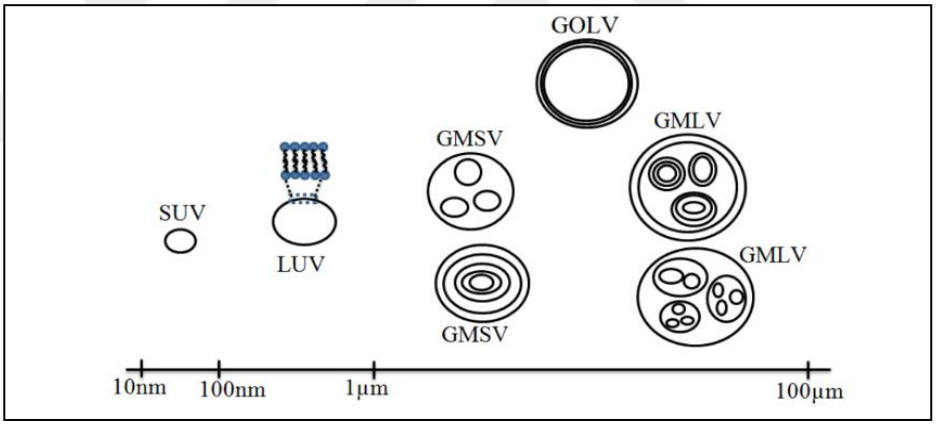

Figure 2.12. Classification of niosome; SUV: Small Unilamellar Vesicle, LUV: Large Unilamellar Vesicle, GMSV: Giant Multilamellar Small Vesicle, GOLV: Giant Oligolamellar Large Vesicle, GMLV: Giant Multilamellar Large Vesicle (41-42, 57-58)

2.4.7. Preparation Methods of Niosomes

1) Ether injection method: This technique was described in 1976 by Deamer and Bangham (3), the Surfactant is dissolved in diethyl ether before being injected into warm water conserved at 60˚ C by a 14 gauze needle. Ether is then vaporized to form single-layer niosomes.

2) Thin film hydration method (Hand shaking technique): surfactant and cholesterol are thoroughly dissolved in an organic volatile solvent (methanol, diethyl ether, or chloroform) in an appropriate size round bottom flask. The organic solvent is eliminated using a rotary evaporator at suitable temperature leaving a solid thin layer on the wall of the flask called film. The dried surfactant film is hydrated later on with the aqueous phase at suitable temperature (0-60˚ C) with gentle shaking typically forming multilamellar Niosomes.

3) Sonication Method: a mixture of drug and surfactant with or without the addition of cholesterol in the buffer is sonicated for 3 minutes at 60˚ C by means of titanium probe producing niosomes.

4) Micro fluidization Method: in which two fluidized streams of surfactant and drug are brought together at extremely high speed in micro channels inside an interaction compartment to form niosomes.

5) Multiple membrane extrusion method: a mixture of surfactant and cholesterol are dissolved in chloroform and then sonicated with PBS. Afterwards drug solution is mixed in to produce a viscous niosome suspension which is thinned by PBS before the organic solvent is evaporated.

6) Remote Loading Technique: thin layer of surfactant/cholesterol mixture is hydrated by citric acid (PH 4.00) by vortexing then frozen and thawed 3 times before sonication. An aqueous solution of the drug is then added and mixed by vortex, then the pH is adjusted by disodium phosphate. Then, this mixture is warmed to 60˚ C for 10 minutes to form niosomes (9).

7) Reverse phase evaporation: Water in oil dispersion is formulated by bath sonicating a mixture of the two phases, and then the dispersion is dried to form a semi-solid gel by means of a rotary evaporator under reduced pressure. Vesicles are formed by the addition of water droplets with vigorous shaking by vortex to form unilamellar vesicles (3).

Niosome size reduction can be achieved by sonication, probe sonication, filtration, extrusion, microfluidization, high-pressure homogenization or a combination of two methods depending on the required vesicle size (59).

2.4.8. Characterization

Morphology: the shape, smoothness, and size distribution of niosomes are frequently elaborated by Scanning Electron Microscopy (SEM) after niosomes are spread on double-faced tape that is fixed on aluminum stubs or on suitable slide (9). Other methods that can be used are freeze fracture replication-electron microscopy (FF-TEM), transmission electron microscopy (TEM), or Light microscopy for vesicles over 1 mm.

Average size, Pdi and zeta potential: can be measured by dynamic light scattering (DLS) instrument, zetasizer, mastersizer, pH-sensitive fluorophores microelectrophoresis, or high performance capillary electrophoresis instruments.

Entrapment Efficiency (EE %): free drug (unencapsulated drug) can be separated from the total amount of drug by centrifugation, dialysis, filtration, or gel chromatography. Both free drug and encapsulated drug (after vesicle destruction) are determined by the applicable analysis method, and the EE% is calculated by the following equation:

$$EE\% = \frac{WL}{WT} \times 100 \quad \text{..... [1]}$$

Or

$$EE\% = \frac{WT-WF}{WT} \times 100 \quad \text{..... [2]}$$

Where WL is the amount of drug loaded in vesicles, WT is the total concentration of drug added to formulation, WF is the concentration of free (unloaded) drug in the dispersion. Eq. [2] is frequently used to measure the EE % when dialysis or centrifugation methods are used for separation (42).

In- vivo and In- vitro studies: differ depending upon the route of administration. They can be investigated by dialysis or permeation through specific filters or by certain test cell cultures (42).

Topical preparations are usually tested with Diffusion Franz Cell using animal tissue such as hairless mouse skin (60), human tissue such as use human cadaver skin, Human skin equivalents which are tissues engineered from a combination of cultured human skin cells together with extracellular matrix components under controlled culture conditions or Artificial membranes such as polysulfone, nitrate mixed ester (61) and cellulose acetate membrane (40) among others.

2.4.9. Applications of Niosomes

The niosomes technology can be used for wide range of applications to treat numerous diseases. The following are some of the many applications of niosomes which are either proven or still under investigation (9).

1) Drug Targeting.
2) Carrying Antineoplastic Treatments.
3) Delivery of drugs used in the treatment of dermal and mucocutaneous infections such as Sodium stibogluconate which is used to treat leishmaniasis.
4) Peptide Drug delivery.
5) Studying Immunological Response.
6) Carriers for Hemoglobin.
7) Transdermal Drug Delivery Systems.
8) Delivery of ophthalmic drugs. (9).

2.4.10. Ultra-deformable Niosomes (UDN)

Elastic, deformable and soft vesicles which have greater capability to improve dermal and transdermal drug delivery than conventional vesicles, introduced first time by Van den Bergh *et al.* (62).

This effect is achieved by modification of the lipid bilayer by introducing substances called edge activators, such as oleic acid, terpenes (44-45), labrasol, cineole, transcutol, diethylene glycol, monoethyl ether (46-47), stearylamine, sephadex-G-100, sodium cholate , sodium deoxycholate and sodium azide, Tween 80, span 80, and span 85 (43, 63).

Certain alcohols like ethanol, propylene glycol or glycerol also act as penetration enhancers when added in specific concentrations (64).

Mechanism of UDN skin permeation: elasticity and deformability of UDN assists them to squash through the channels of the stratum corneum which are less than one tenth of their own diameter. Thus, the actual model that describes transport UDN comprises complex theoretical submerging of ‘elasto mechanics', material transport and hydration/osmotic force (65). This mechanism of UDN skin penetration is shown in Figure 2.13.

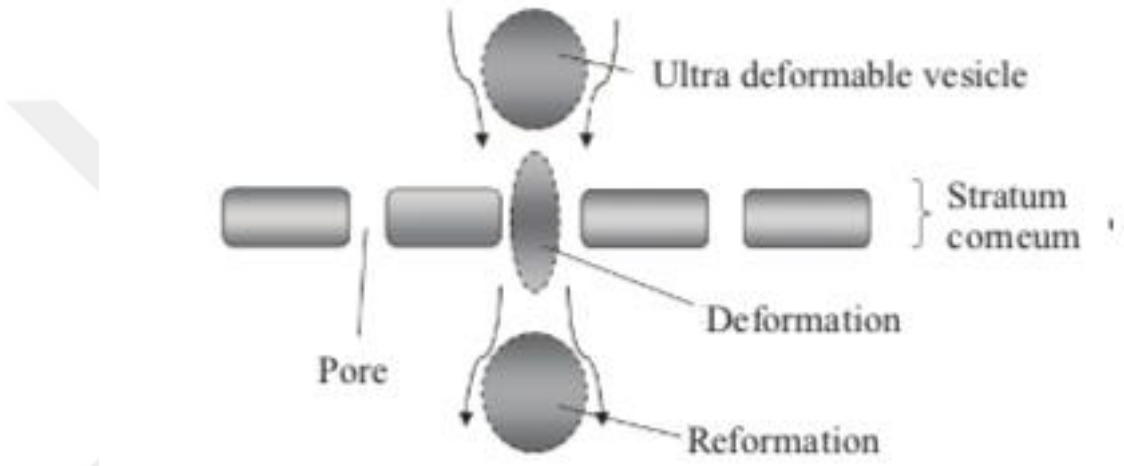

Figure 2.13. Mechanism of skin permeation by UDN (65)

2.5. Franz Diffusion Test

The Franz Cell chamber is an apparatus used to test in vitro skin permeation. It is recurrently employed in topical formulations development. It comprises two primary chambers separated by a membrane. The formulation to be tested is spread over the membrane thru the top chamber, while the bottom chamber holds the fluid media from which samples are removed at ordered time intervals for analysis. This analysis helps to reveal the amount of active substance that has permeated the membrane through time. The temperature of the chamber is maintained constant through the analysis time. Although giving a perception of permeability, results of the Franz cell test does not certainly predict the efficacy of a formulation in vivo; it does allow, though, to conclude whether the formulation transports an active ingredient through the skin (66).

Franz Cells diffusion is a broadly used method to estimate in vitro permeation of a drug [3, 5, 6], it's advantageous as it requires:

- √ minimal tissue handling
- √ no continuous sample withdrawal
- √ small amount of the material to be tested (67)

The following testing parameters are to be considered:

Volume: the true volume of each receptor chamber should be measured before running the test. This is to be done with the internal stirrer placed inside.

Temperature: The receptor medium's temperature must be kept constant within 1.0 ^{o}C of the target temperature throughout the test.

Speed: The speed of rotation must ensure sufficient blending of the receptor media during the test. Its acceptance is 10% from the aimed speed (typically 600–800 rpm).

Sampling Time: Samples should be removed at the determined time(s) with an acceptance +/- 2 min.

Validation: The validation of the apparatus is confirmed by proving that the test temperature and rotation requirements are met; alongside performance verification test (PVT), unless else specified by the individual monograph. The PVT is passed when 2 of 6 cells meet by 90% confidence interval with the terms of FDA's SUPAC-SS requirements. The PVT is implemented by an analyst to test the required reference standard two times, where the first test performed with 6 cells is outlined as the reference. And the second test of 6 cells is outlined as the test. The PVT is approved if the second test exceeds the 90% confidence interval with allusion to the reference test (68-69).

2.5.1. Procedure

Unless elsewise detailed in the individual monograph, the used media should be degassed by means of a suitable technique. Stirrers are placed in the chambers before filling them with the media and letting them come to the required temperature. If needed, the membrane is allowed to be saturated in the media for 30 min or as required according to the type of the membrane. The membrane is placed on the donor compartment before it is flipped. The test material is then applied into the void of the

donor compartment, and dispersed to cover the whole surface of the membrane. Each of the ready dosage compartments is fitted to each cell with the membrane in contact with the receptor media, ensuring that there are no bubbles under the membrane. Once ready, the stirring device is turned on, which represents time zero. The required sampling method is followed, collecting a sample from each cell for further analysis and replacing the removed amount with fresh media, but no bubbles should be introduced into the cell during the sampling and replacing process (68-69).

2.5.2. Calculations

Flux (J) is defined as the quantity of permeant traversing the membrane per time per unit area; expressed as quantity/area/ time. The following formula can be used to calculate flux only if the permeant was used in a predetermined dose:

$$J = \frac{Q}{A \times t}$$

Where Q is the amount of permeant crossed the membrane in time t, while A is the area of membrane subjected to the permeant in cm^2.

Steady state flux (Jss) is deemed when the concentrations at consecutive sample withdrawal intervals are not considerably different. The flux at this point is steady state flux. Therefore, it can be defined as the quantity of permeant traversing the membrane at a constant rate.

Permeability constant (Kp) is described as the flow rate of a liquid or gas across a permeable barrier and expressed in cm/min or cm/hr. It can be calculated by the equation:

$$K_p = \frac{Q}{A \times t \times (C_0 - C_i)}$$

Where Q is the amount of permeant transmitted through the membrane in time t

Ci and Co are the concentrations of the permeant on the receptor side and the donor side respectively.

A is the area of membrane subjected to the permeant in cm^2 (61, 70).

2.5.3. Method Development

The membrane with which Franz diffusion cell system (Figure 2.14) is operated can be a tissue assembly, synthetic membrane, or a biological sample. This membrane

comes in between the donor compartment which holds the material to be tested and the receptor compartment containing the appropriate medium. Phosphate Buffered Saline (PBS) is usually the medium of choice (68-69).

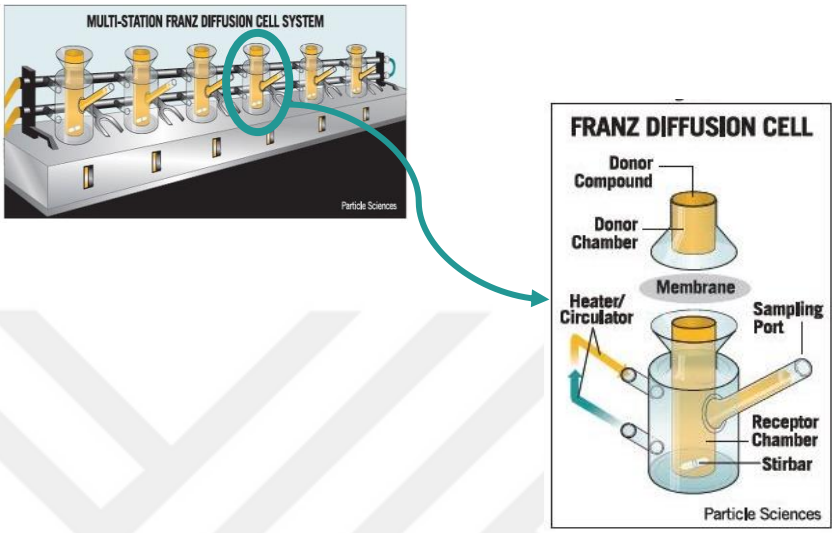

Figure 2.14. Franz diffusion cell (68-69)

SUPACSS2 offers a logical starting point for the receptor medium: “Applicable receptor medium such as hydro-alcoholic medium for sparingly water-soluble drugs or aqueous medium for water soluble drugs” can be employed (68-69). Therefore, after creating an essential assay method, the first mission is measuring the solubility of the active substance in numerous solvents varying from aqueous solutions like PBS to hydro-alcoholic solutions like isopropanol/PBS-50/50 (v/v). The purpose is to distinguish solvents that grant sink conditions in the receptor chamber (68-69).

Occasionally, two choices for the medium can be engaged: one for quality control purposes like manufacturing process change control and long-term stability tests. In such a case, a non-physiologic medium might be utilized; the other is a physiologically relevant media employed to mimic in vivo behavior. The latter could be

beneficial for establishing a prospective in vitro – in vivo correlation (68-69).

2.5.4. Membrane Choice

There are numerous varieties for membranes extending from tissue constructs, freshly excised tissue, and body tissue to synthetic membranes. Considerations affecting the choice of the appropriate membrane involve compatibility with the material to be tested, cost, reproducibility, availability, and most decisively, the target of the research. Synthetic membranes differ in thickness, hydrophilicity and pore size. Because water is the key component of several semisolid formulations, synthetic membranes which are hydrophilic or hydrophilized are classically used (68-69). Illustrative IVRT parameters of permeability test is shown in Table 2.4.

2.5.5. Sampling

Several sampling times throughout a suitable time interval to create an acceptable release profile (e.g. 30 min, 1, 2, 4 and 6 hours) are commonly recommended. The “burst effect”, a repeatedly seen phenomenon where an excessive initial release occurs, along with the time of release determine the sampling times. It is also not unusual to prolong the run to 24 hr relying on the intended clinical usage and anticipated investigational data.

Other parameters, such as, the type of diffusion cell, the membrane diameter, the amount of tested product, and aliquot withdrawn from the receptor vessel Are endorsed by SUPAC-SS (68-69).

Table 2.4. Illustrative IVRT parameters (68-69)

ILLUSTRATIVE IVRT PARAMETERS	
Diffusion cell	9-station Franz cell stirrer
Weight of sample gel	0.2 – 0.4 g
Membrane	Hydrophilic membrane, 25 mm diameter, 0.45 µm pore size
Receptor medium	PBS based
Temperature	32 °C or 37 °C (Vaginal products)
Stirbar speed	600 rpm
Sampling aliquot	200 - 400 µL
Sampling time	0.5, 1, 2, 3, 4, 6 hr
	Particle Sciences

As demanded by SUPAC-SS2, the data output is a summary of the release rates (µg/cm2 · √hr) throughout a brief period (e.g. 4 or 6 hours, any that offers a straight line for release profile). Figure 2.15 (a) and (b) shows a classic release profile.

(a)

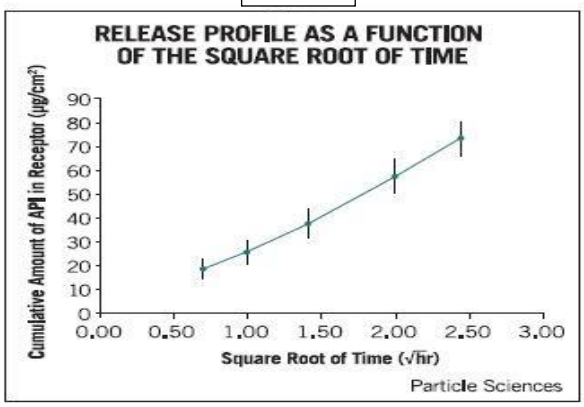

(b)

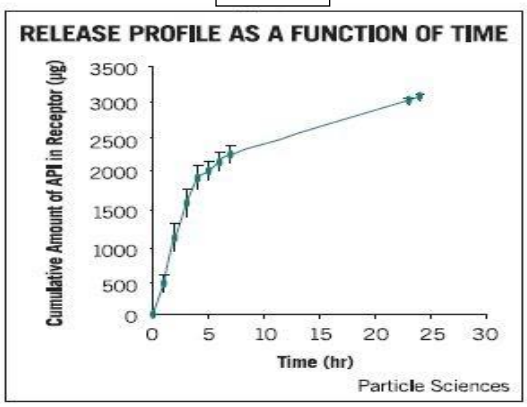

Figure 2.15. Classical release profile; a: release profile as a function of square root of time, b: release profile as a function of time (68-69)

Moreover, other values such as the material's permeability (cm/hr), flux rate (μg/cm^2 hr), and 24-hr accumulation (μg/cm2) can additionally be reported, which offers a comprehensive picture of material's release and accumulation. Figure 2.15 (b) demonstrates the cumulative amount of a material as a function of time, where the slope of the linear portion (the steady state) represents the flux of the substance, and the Y-axis tags its accumulation at specific time (68-69).

2.5.6. Possible Artificial Membranes

- ✓ Hydrophilic polysulfone membranes (Tuffryn®; Pall Corporation, Port Washington, NY, USA) (4)
- ✓ Cellophane membrane with molecular weight cutoff, 12,000 to 14,000 (HIMEDIA, India Ltd) (71)
- ✓ Cellulose membranes for dialysis, (Sigma-Aldrich USA) (67)
- ✓ Strat-MTM membranes (Millipore Temecula, MA, USA) (67)
- ✓ cellophane membrane (72-73)

2.5.7. Strat-M^{TM} Membrane

This is an artificial polymeric membrane utilized for dermal permeation testing. It is more extrapolative for diffusion and permeation in human skin devoid of variability, safety and storage restraints (74).

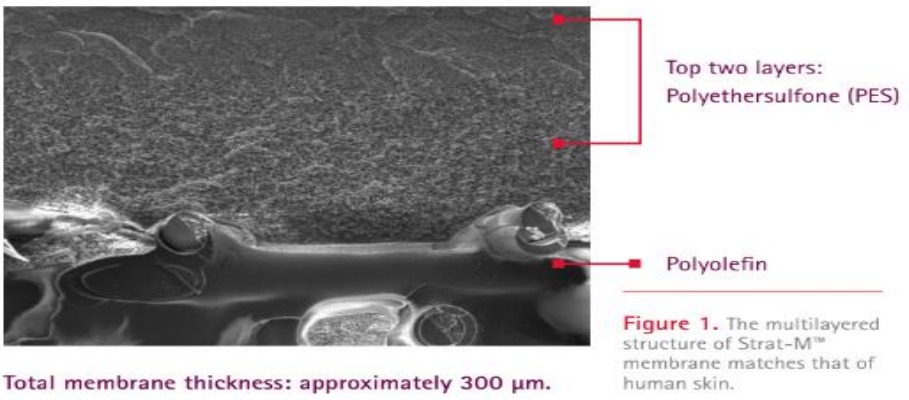

Figure 2.16. Structure of Strat-M^{TM} membrane (75)

As revealed in Figure 2.16., It is fabricated of two layers of polyethersulfone (PES, less diffusive) fixed over a layer of polyolefin (which is more diffusive). A porous construction with a gradient throughout the membrane in terms of pore size and diffusivity is created with these polymeric layers. The porous structure is infused with a patented exclusive mixture of synthetic lipids, conveying extra skin-like properties to the synthetic membrane, making diffusion across Strat-M membrane predictive of diffusion through human skin for a widespread variety of substances such as Active pharmaceutical and cosmetic ingredients, Chemicals, Formulations, Personal care products, and Pesticides (75).

Strat-M membrane is more correlated to human skin (Figure 2.17) than animal skin are in maximum cases. The flux of 14 investigation compounds extending in molecular weight from 162 to 425 having log P values of -0.131 to 6.9 representing relative lipophilicity through human skin and Strat-MTM membrane, reveal that Strat-M membrane has wide chemical compatibility making it a great model for screening compounds with various physicochemical properties (75).

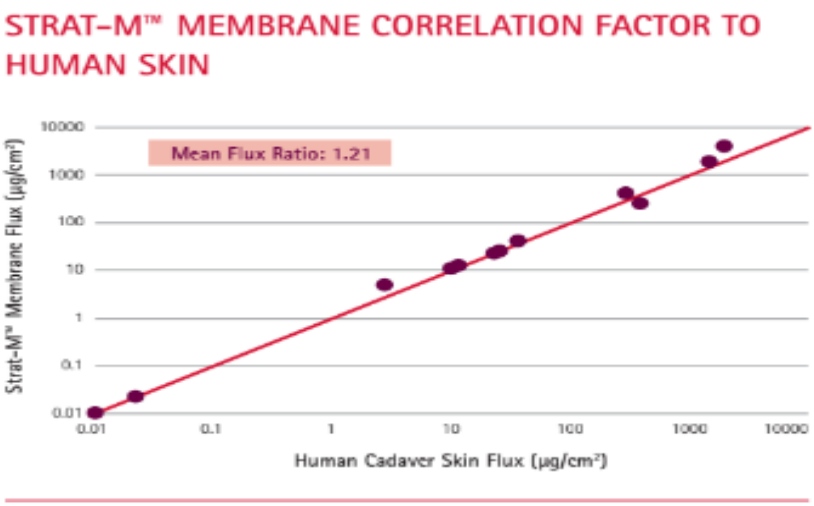

Figure 2.17. Evaluation of flux through Strat-M membrane skin vs. through human. Data points represent the ratios of average values of accumulative flux of several materials through human cadaver skin and Strat-M, deliberated at 8 hours. The solid line denotes the ideal 1:1 correlation. N = 14 (75).

Permeability studies using Strat-M membrane exhibits a reproducible method, which is easy to put into practice for the preformulation stage or to evaluate the functioning of semi-solid pharmaceutical or cosmetic products for transdermal or topical application (67). As the permeability of Strat-M is found comparable to that of the skin, Strat-M membrane can be functional as an economical and stable membrane to distinguish between the permeation of lipophilic and hydrophilic compounds in initial stage studies of diffusion and permeation for transdermal formulations. Strat-M membrane has a uniform structure abolishing the inconsistency characteristic in both skin and other polymeric membranes such as cellulose acetate. In addition, its use is simple and involves no pretreatment (76).

3. MATERIALS AND METHODS

3.1. Materials and Equipments

3.1.1. Materials

The materials used in this study are given in Table 3.1.

Table 3.1. List of Materials

Material	**Company**
Cholesterol	Merck, Germany
Methyl laurate	Sigma-Aldrich, Germany
Potassium chloride	Sigma-Aldrich, Germany
Potassium diphosphate	Riedel-de haen, Germany
Serenoa repens extract	Sigma-Aldrich, Germany
Sodium chloride	Sigma-Aldrich, Germany
Sodium cholate	Sigma-Aldrich, Germany
Sodium monophosphate	Riedel-de haen, Germany
Span 60	Sigma-Aldrich, USA
Tween 60	Merck, Germany

3.1.2. Equipments

The equipmenst used in this study are listed in Table 3.2.

Table 3.2. List of Equipments

Equipment Names and Models	**Company**
Diffusion Franz cell	Permegear, USA
Extruder	Liposofast, Canada
HPLC	Agilent, USA
Magnetic stirrer	Isolab, Germany
Polycarbonate filter, Whatman® Nuclepore Track-Etched	Sigma-Aldrich, Germany
Probe sonicator	Bandelin, Germany
Rotary evaporator	Heidolph, Germany
Scanning electron microscope	ZEISS EVO 40
Sputter Coater	Leica EM ACE200
Viscometer	Brookfeild, USA
Vortex	Scilogex, USA
Zeta-sizer	Malvern, UK

3.2 Methods

3.2.1. Preparation of Phosphate Buffered Saline (PBS)

Phosphate Buffered Saline (PBS) was prepared using the constituents listed in Table 3.3 concurring with the Cold Harbour Spring Phosphate Buffered Saline Protocol (77) with slight modification for pH adjustment to 5.5.

Table 3.3. Composition of PBS

Components	Amounts, g
Sodium monophosphate	1.44
Potassium diphosphate	0.24
Sodium chloride	8.00
Potassium chloride	0.20

The above-mentioned components were dissolved in distilled water and the volume was completed to just below 1 L. Then, the pH was measured with a calibrated pH meter and adjusted to 5.5 with acid or base. Finally, the volume was completed to 1 L.

3.2.2. Establishment and Validation of Calibration Curve for Methyl Laurate

Construction of Calibration Curve

HPLC methods developed by guarrasi et al. (78). A calibration curve was prepared using 1, 0.5, 0.25, 0.1, 0.05, 0.02 mg/mL of ML in mobile phase. These series of concentrations were prepared from a stock solution of 50 mg/mL. For each point, 3 replicates were used. Calibration curve was obtained by plotting the average peak area for each point against the concentrations. The conditions used for HPLC analysis are given below.

HPLC Conditions:

- Column: Eclipse XBD-C18 4.6 mm ID x 250 mm (5μm) 80A
- Autosampler: Thermostat set at 25 °C
- Column (analysis) Temperature: 25 °C
- Quaternary pump: set to deliver 1.00 mL/min
- UV Detector: set at 208 nm
- Injection volume: 20 μL

• Isocratic Mobile Phase: 90:9.8:2 (v/v) mixture of acetonitrile, methanol and n-hexane acidified with 0.2% acetic acid.

Validation of Analytical Method for ML

The method was validated by determining the following validation characteristics: linearity, sensitivity, accuracy, precision, specificity and stability.

Linearity

The linearity of an analytical method is its capability (in a given range) to obtain test results directly proportional to the concentration of analyte in the sample. Linearity was established using a six-point (1, 0.5, 0.25, 0.1, 0.05, 0.02 mg/mL) calibration curve, with 3 replicates for each point. Average peak area for each concentration point was plotted against Methyl laurate concentration. Linearity was confirmed by calculation of a regression line by the method of least squares and by visual inspection of the plot.

Sensitivity

Sensitivity of the method was concluded by finding the detection and quantitation limit. The detection limit is verified by the analysis of ML samples with identified concentrations and by determining the lowest level at which the ML can be consistently detected. The signal-to-noise ratio was implemented by comparing calculated signals from samples with specific low concentrations of ML with those of blank samples (mobile phase). Least concentration at which a signal-to-noise ratio was 3:1 was accepted as the detection limit. Least concentration at which a signal-to-noise ratio was 10:1 was accepted as the quantitation limit.

Accuracy and Precision

For evaluating intra-day and inter-day (3 consecutive days) accuracy and precision, samples of 3 known concentrations (0.75, 0.4, and 0.075 mg/mL) prepared from a stock solution of 50 mg/mL in mobile phase were analyzed with 3 replicates (n = 3) for each. Precision, on the other hand, was deliberated by the coefficient of variation.

Accuracy was calculated by the following equation:

$$Accuracy = \frac{C_f - C_a}{C_a} \times 100$$

where, C_f = Average found concentration calculated by regression equation

C_a= Added concentration.

$$Precision = \frac{\sigma}{\mu} \times 100$$

where, σ = Standard deviation

μ = Mean of repetitions.

Specificity

ML and niosomal ML Solution and their corresponding blank samples were dissolved/diluted in mobile phase and were analyzed. Chromatograms were compared to see whether any changes arise on the retention time of ML or enough resolution is possible so that ML peak is not disturbed by any other substances.

Stability

Stability of ML in the analytical conditions was verified by dissolving ML in mobile phase (25 and 100 mg/mL) and exposing to 25°C for 30 minutes, the analysis time being 5 min. 30 minutes later the samples were analyzed and modifications in retention time or presence of extra peaks were inspected.

3.2.3. Preparation of Niosomes

Niosomes were prepared by thin film method (9, 56). A mixture of surfactant, cholesterol, and either ML or SPE were dissolved in a mixture (2:1 ratio) of chloroform and methanol in a 100 mL round bottomed flask. Then, the solvent mixture was evaporated in a rotary evaporator at 100 rpm with a temperature of 45^{o} C under a pressure of 315 mbar, reduced to 115 mbar after about 20 minutes to create a thin film which is left in desiccator overnight to ensure complete removal of organic solvent. Next day, the film was hydrated using PBS at 60^{o} C, which is above the transition temperature of surfactant 53^{o}C (79-80), for 60 minutes by magnetic stirrer followed by bath sonication for 15 minutes. This was left at room temperature until the next day in order for the vesicles to mature. The niosome dispersion was vortexed for 1 minute at maximum speed, and then this was extruded through a 400 nm polycarbonate filter. The extrusion was repeated 10 times on each sample. The overall process is shown in Figure

3.1. Elastic niosomes were prepared in the same manner with the addition of 0.13 mM of sodium cholate together with other ingredients before dissolution by chloroform/methanol mixture (81-82).

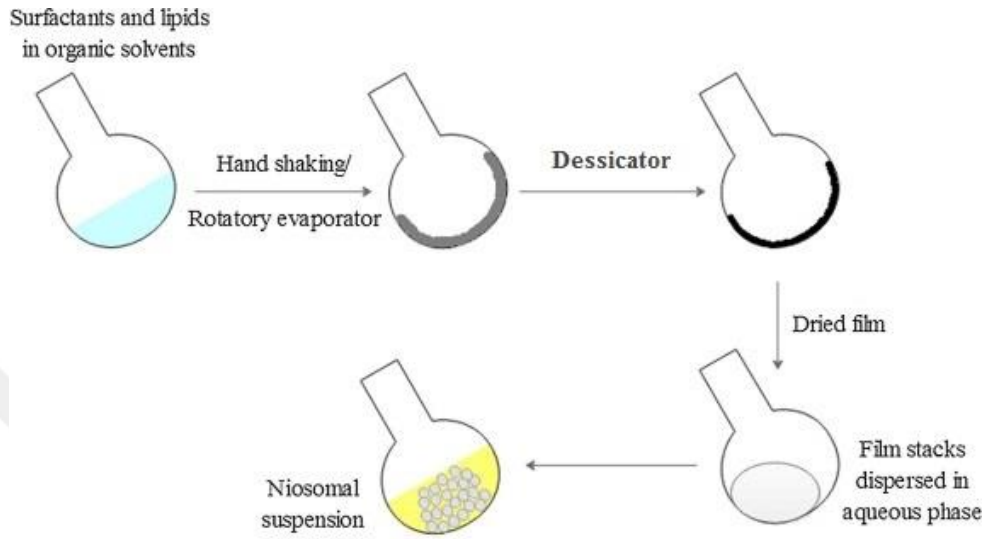

Figure 3.1. Schematic diagram of the preparation of niosomes using thin film hydration method (56)

3.2.4. Optimization of Formulation and Process Variables

Formulation and process variables were optimized using ML niosomes through two stages, first, by assessment of film formation, then by dispersion quality and vesicle size.

Film formation was examined by the following variables:

- **Surfactant**: two different surfactants Span 60 and Tween 60 and a 50:50 (mM by mM) mixture of both were tested.
- **Cholesterol to surfactant ratio:** 0:1, 0.5:1, 1:1, and 1:1.5 molar ratios were tested.
- **ML to Surfactant ratio**: 0, 1, 2, 2.5, 4 mg of ML to 1 mM surfactant were tested.

- **Evaporation temperature:** different evaporation temperatures 20, 45, 55, 70, 80^{o} C were tested during film formation by solvent evaporation.
- **Evaporator rotation speed:** different rotavapor speeds 70, 80, 90, 100, 120 rpm were tested during solvent evaporation.

Dispersion quality and vesicle size were examined by changing the following variables:

- **Cholesterol to surfactant ratio.**
- **Hydration temperature**: different temperatures (55, 60, 80˚C) were applied while hydrating films.
- **Hydration method**: two methods for film hydration were tested magnetic stirrer and rotation in rotary evaporator without applying pressure.
- **Hydration time**: the determined hydration method was applied to different formulations for 20, 40, 60 minutes to see the time effect on dispersion quality and vesicle formation.
- **Size reduction method**: either bath sonication, probe sonication, extrusion or a combination of two or more methods were tested.

3.2.5. Characterization of Niosomes

Size and Zeta-potential

Vesicle size was measured by dynamic light scattering method. Zeta-potential was measured by the technique of laser Doppler velocimetry and phase analysis light scattering (PALS). For this purpose, 50 µL of the vesicle suspensions were diluted to 1 mL with purified water. This diluted dispersion was put into the size measurement cuvette and the cuvette into the Zeta-Sizer machine for taking the reading. Special cuvette with in-built electrodes was used for measuring the zeta-potentials of the vesicles.

Scanning Electron Microscopy

The morphology of vesicles was visualized by scanning electron microscopy, SEM. One drop of each of the optimized formulations was placed on a glass slide and

left to dry at room temperature overnight. After drying, the vesicles were silver coated in a sputter coater. This was then observed in a scanning electron microscope.

Qualitative Entrapment Capacity

Entrapment efficiency is the amount of active substance which is loaded/entrapped into the vesicles as a percentage of the added amount of active to the formulation (42). Entrapment capacity expresses the ratio of active substance to the surfactants amount. Because of the difficulty in the separation of similar density niosome and extract or ML, entrapment ratio was determined with an alternative qualitative approach. With a fixed formulation (as for empty niosome), different amounts of ML or SPE were added and dissolved in chloroform-methanol solvent mixture. Then, the solvent was evaporated and a thin film formed. Occurrence of yellowish unmixed spots (ML) or greenish spot (SPE) in the film clearly indicated the presence of unentrapped drug. This was further confirmed by observation of large vesicles in hydrated film under light microscope. In samples with too much ML or SPE, unentrapped chunks of ML or SPE were observed. The highest amount which just showed no such unentrapped ML or SPE was taken for subsequent study. The ratio of ML or SPE to the surfactant at this level is defined in this study as entrapment capacity.

Elasticity/Deformability

The measurement of elasticity (deformability) of deformable vesicles was carried out by extrusion technique. After film hydration, initially formed large vesicles were extruded through a 400 nm polycarbonate filter enough number of times to achieve on an average 400 nm size vesicles. The vesicles were then extruded through a 200 nm polycarbonate membrane filter at constant pressure. The elasticity of the vesicles is then expressed in terms of deformability index according to the following equation (83-84). According to this, vesicles which are elastic or deformable tend to maintain their average size after extrusion through a smaller pore size membrane than the vesicle size, and such deformability index remain close to unity. The related equation is as follows:

$$DI = \frac{S_b}{S_a}$$

where

DI is deformability index;

S_b is the size of vesicles before extrusion

S_a is the size of vesicles after extrusion

Stability

Initial stability studies formulations were tested after storing samples for 7 days at 4-8º C (refrigerator) and at room temperature for vesicle appearance and vesicle size. Niosomes were not stable at room temperature, so room temperature or higher temperatures was not included in the later experiments. The optimized formulations for both ML and SPE were tested 1 month, 2 months, and 4 months after preparation while storing at 4-8˚ C.

Permeability

Permeability study was performed by Franz Diffusion Cell. Since ML is a major component of the SPE and it was chosen from the beginning of this study as a representative for the extract, permeability study was performed on ML formulation only for the ease of analysis. Two studies were performed, one comparison study for 2 different membranes: 0.45 µm nylon filter and Strat-M membrane. For this one-point sampling at 6h was performed. This was done to compare different types of membranes. For the main permeability study with Strat-M membrane multipoint sampling was performed as shown in Table 3.4. The parameters for each study are also detailed in Table 3.4.

Table 3.4. Permeation study parameters

Diffusion cell	Six-station Franz Cell
Amount of sample	1.5 mL
Concentration	2 mg/mL
Membrane	Nylon filter 0.45 µm Strat-M membrane
Membrane diameter	47 mm
Receptor medium	PBS pH 5.5
Volume of receptor chamber	20 mL
Temperature	32º C
Sampling aliquot	1 mL
Sampling time	0, 2, 4, 6, and 8 hours

Aliquots were dried at 60˚C by nitrogen gas blow until complete dryness, and then the dried samples were dissolved by 0.5 mL of mobile phase before being analyzed by HPLC, thus giving a concentration factor of 2. Flux, permeability and cumulative amount permeated per cm^2 were calculated for each time point. Cumulative quantity permeated per cm^2 was charted against time and the slope of the linear part was calculated to define the Steady State Flux.

3.2.6. Incorporation of Niosome into Gel Preparation

The optimized niosome formulations containing either ML or SPE were incorporated into gel formulations prepared from sodium carboxymethyl cellulose (Na-CMC). Two more gel formulations, one with added empty niosome and another blank gel without any added niosome were prepared for comparison purpose to see how the addition of loaded niosome might affect the gel formulation. The formulations of the gels are listed in Table 3.5.

Table 3.5. Niosome incorporated gel formulations

Ingredients	**Amounts %, w/w**			
	MLnioG	**SPEnioG**	**BLANKnioG**	**BlankG**
CMC-Na	4.00	4.00	4.00	4.00
Glycerin	2.50	2.50	2.50	2.50
Methyl paraben	0.05	0.05	0.05	0.05
Propyl paraben	0.05	0.05	0.05	0.05
ML Niosome	20.00	-	-	-
SPE Niosome	-	20.00	-	-
Unloaded Niosome	-	-	20.00	-
PBS (pH= 5.5)	q.s. 100	q.s. 100	q.s. 100	q.s. 100

The gel preparations were prepared by weighing all the ingredients, except niosome, in a clean beaker. Then PBS was added and stirred with a magnetic stirrer for 30 minutes until complete dissolution and gel formation. Finally, niosome formulations were added at 20% w/w concentration.

3.2.7. Evaluation of Niosome Gel Preparations

All gel preparations were evaluated for pH, density, and rheological properties. pH were measured with a calibrated pH meter without dilution of gels. Densities were determined by weighing 5 mL of gels minimizing air bubbles within the gels. Viscosities were measured by a Brookfield viscometer. Shear rates were applied between 1 to 50 cm^{-1} and corresponding shear stress and viscosities recorded. Finally, correlation between shear rate and shear stress were determined from the linear portions of each rheogram. If strongly correlated, plastic viscosities were found from the slopes of the trend lines.

4. RESULTS

4.1. Quantitative Determination of Methyl Laurate by HPLC

Quantitative determination of ML was performed under the conditions described in section 3.2.2 a representative HPLC chromatogram of ML and SPE are given in Figure 4.1 and 4.2 respectively.

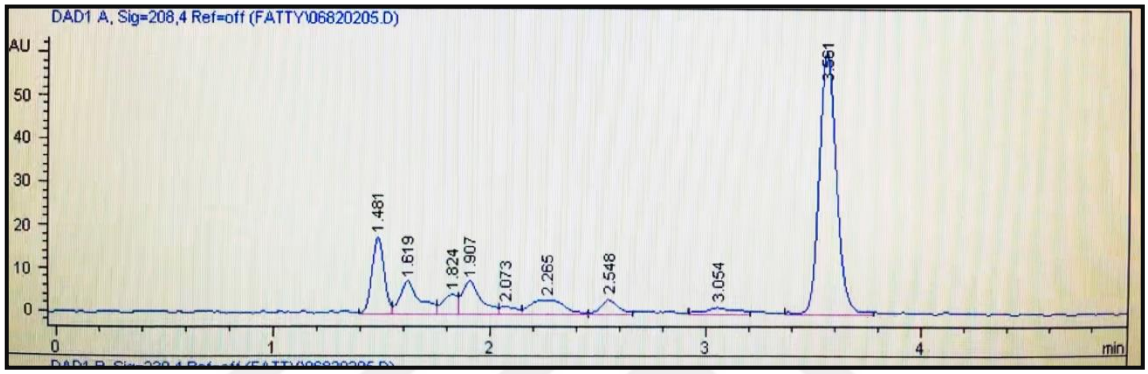

Figure 4.1. HPLC chromatogram showing ML peak at 3.5 minutes

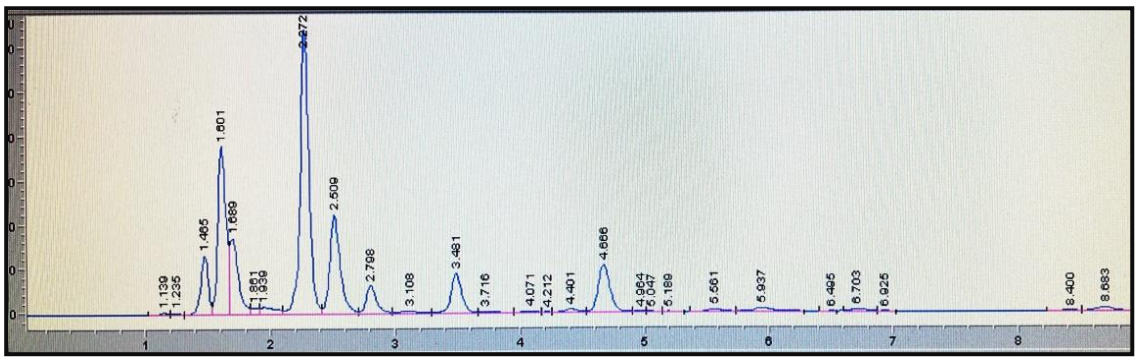

Figure 4.2. HPLC micrograph showing SPE spectrum with ML peak appearing at 3.5 minutes

4.1.1. Methyl Laurate Calibration Curve

ML calibration curve was constructed concurring to the method explained in the section 3.2.2. The calibration curve is given in Figure 4.3. The slopes from different series were calculated and the variation coefficients of these 3 slopes were found to be 331.2 The average values of the slopes and intercepts, along with other analytical data, are given in Table 4.1.

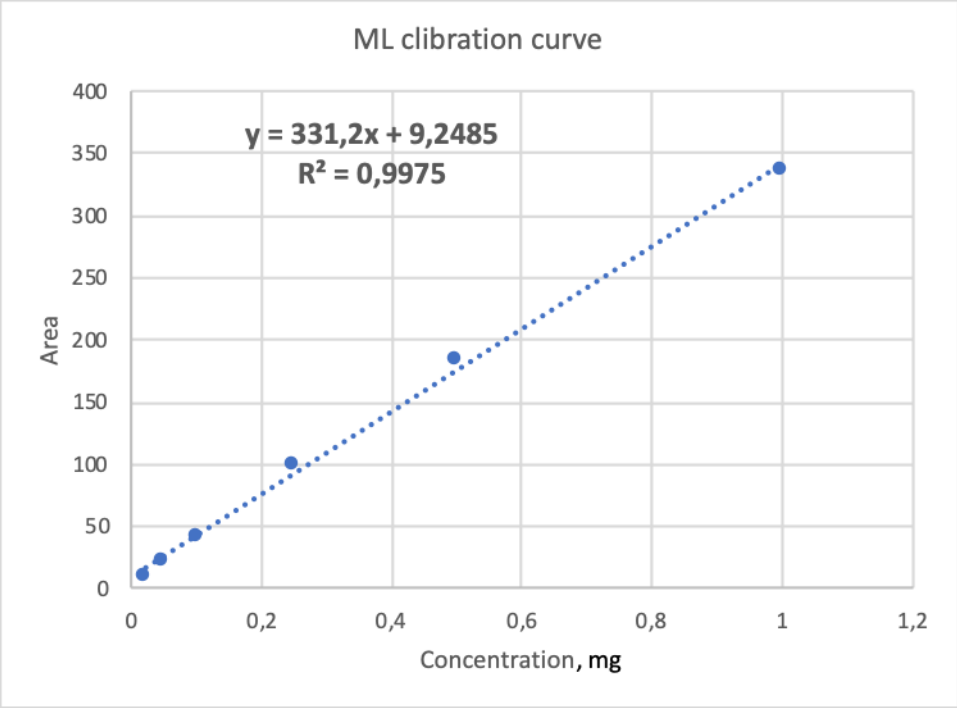

Figure 4.3. ML calibration curve

Table 4.1. Linear regression data (n=3) obtained in HPLC analysis of ML**.**

Parameter	Result
Concentration range	0.02 - 1 mg/mL
Slope	331.2
Intercept	9.2485
Correlation coefficient	0.9995
Detection limit	0.003
Quantification limit	0.01

4.1.2. Validation of Analytical Method for ML

Linearity and Sensitivity

Visual inspection of the ML concentration vs peak area plot clearly shows a linear curve over the range of 0.02-1 mg/mL with correlation (fitness) coefficient (0.9995).

As described in section 3.2.2., detection limit (signal-to-noise ratio was 3:1) and quantitation limit (signal-to-noise ratio was 10:1) of ML were found to be 0.003 and 0.01 mg/mL, respectively.

Accuracy and Precision

As described in section 3.2.2., three standard concentrations (0.75, 0.4, and 0.075 mg/mL) of ML from the range of calibration curve were prepared and analyzed with 3 replicates (n = 3) for each of these three concentrations for assessing intra-day and inter-day (3 consecutive days) accuracy and precision. Accuracy and precision data are shown in Table 4.2.

Table 4.2. Accuracy and precision data

	Added Concentration mg/mL	**Found concentration mg/mL**	**Accuracy (%)**	**Precision (Coeff. of variation, %)**
Intra-day	0.75	0.795	6.00	8.87
	0.40	0.423	5.75	10.89
	0.075	0.073	-2.28	6.38
Inter-day	0.75	0.798	6.50	11.91
	0.40	0.426	6.68	9.82
	0.075	0.080	6.67	11.76

Following the calculation as described in section 3.2.2, accuracy was found to be in the range between -2.28 and 6.68. Precision was found to range between 8.87 and 11.91. Intra-day and inter-day accuracy are shown in Figure 4.4.

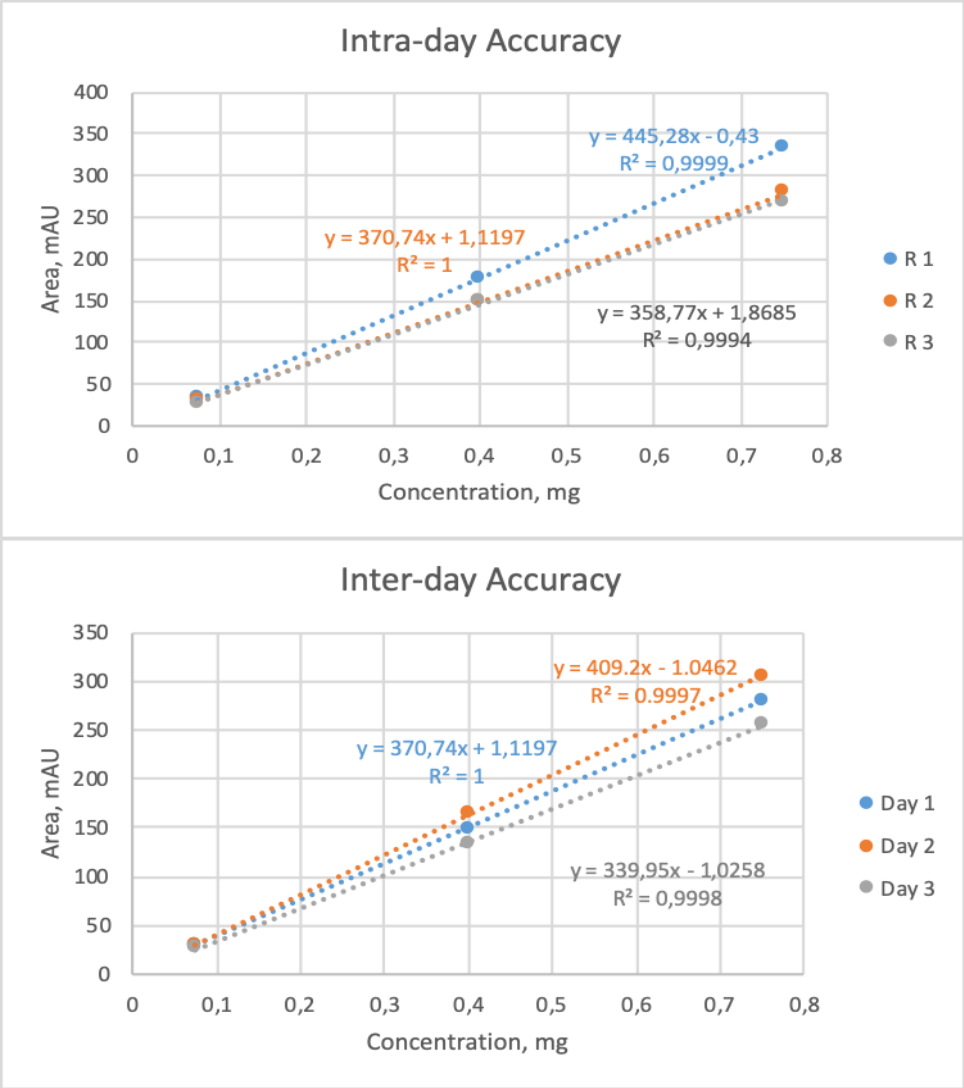

Figure 4.4 Intra-day (top) and inter-day (bottom) accuracy chart (n=3)

4.2. Optimization of Formulation and Process Parameters

4.2.1. Effect on Thin Film

Surfactant Types

Both Span 60 and the 50/50 (mM by mM) mixture of Span 60 and Tween 60 formed very good films. While Tween 60 alone did not form a film at all with ML, instead, it formed a very thick oily mixture at the bottom of the flask. Span 60 formed very rigid vesicles, which could not be extruded. Therefore, Span 60-only niosome were discarded from further studies.

Cholesterol to Surfactant Ratios

Effect of cholesterol to surfactant ratios on thin film formation and vesicle size are shown in Table 4.3. The best film in the sense of homogeneity, smoothness, easiness of formation, and reproducibility with ML was the 1:5 ratio, which also formed better dispersion and smaller vesicle size later on.

Table 4.3. Effect of cholesterol to surfactant ratio on thin film formation, dispersion quality and vesicle size

Cholesterol:Surfactant mM/mM	Quality of thin film	Dispersion quality	Average vesicle size, nm*
0:1	Good, smooth film	Nonhomogeneous, unstable.	-
0.5:1	Good, smooth film	Homogeneous, stable.	821
1:1	Bad, rough film	Nonhomogeneous (clump)	-
1:5	Good, smooth film	Homogeneous, stable.	519
3:7	Good, smooth film	Homogeneous, unstable.	775
4:6	Bad, rough film	Nonhomogeneous (clump)	-

*Vesicle size was measured after bath sonication for 30 minutes; size measurement was done only for homogeneous stable dispersion formulations

ML to Surfactant Ratio

While the amount of surfactant was kept fixed at 0.1 mM, the amount of ML was increased gradually until oily spots started to appear in the film which indicated unincorporated ML as mentioned in section 3.2.4. The maximum amount of ML that could be added without spotting was found to be 2 mg ML per 0.1 mM surfactant.

Evaporation Temperature

The most convenient evaporation temperature was found to be 45˚ C as it evaporates the organic solvents mixture slow enough to form a smooth film without bubbling or boiling.

Rotation Speed

Ninety to 100 rpm was found optimum for good film formation. Slower speed leads to the formation of an uneven film which was thicker at some places than others, while faster speed causes the solvent mixture to boil causing the film to be rough.

4.2.2. Effect on Dispersion Quality and Vesicle Size

Cholesterol to surfactant ratio

As shown above (Table 4.3), cholesterol to surfactant ratio of 1:5 was opted for the optimized formulation because it resulted in homogeneous and stable dispersion with acceptable vesicle size.

Hydration temperature

Sixty degree Celsius was opted for further formulations since it resulted in the most homogenous dispersion that started to form soon after the PBS was added and remained homogenous for at least 30 days later.

Hydration Method

Rotation in rotavapor during hydration was abandoned as the dispersion formed by this method was nonhomogeneous and chunky. On the other hand, stirring by magnetic stirrer at 300 rpm resulted in homogeneous emulsions.

Hydration Time

Stirring the dispersion for 60 minutes by magnetic stirrer after the addition of PBS was found ideal for the formation of homogeneous and stable dispersion. Less time resulted in unstable emulsions which sedimented or became chunky soon, while more time did not have any further advantage.

Size Reduction Method

Bath sonication caused a size reduction to not less than around 500 nm. In addition, applying it for more than 30 minutes lead to dispersion disruption. Probe sonication for more than 3 minutes in room temperature increased the temperature of the formulation excessively causing dispersion disruption, this problem was resolved by placing the dispersion in ice bath while sonicating. However, the minimum size achieved by this method was around 500 nm. Bath sonication followed by probe sonication did not result in better size reduction. Extrusions through 400 nm polycarbonate filter for 10 times gave the best results, producing vesicles as small as 185 nm.

The following table (Table 4.4) shows different set of variables that were applied in the experiments.

Table 4.4. Formulation and process variable sets used in the optimization study

Parame-ter Sets	**Surfactant**		**Chol, mM**	**Na Cholate, mM**	**Evapo. Temp.˚ C**	**Hydration**		**Size Reduction**	
	Type	**Conc mM**				**Tem. ˚C**	**Time, min**	**Method**	**Time, min**
Set 1	Span 60	0.1	0.1	-	40	-	-	-	-
Set 2	Span 60	0.1	0.05	-	40	55	30	Bath sonic.	20
Set 3	Span 60	0.1	0.05	-	40	55	30	Bath + probe	20+10
Set 4	Span 60	0.1	0.1	-	60	-	-	-	-
Set 5	Span 60	0.7	0.3	-	25	70	20	Bath	20
Set 6	Span 60	0.6	0.4	-	25	-	-	-	-
Set 7	Span 60	0.5	0.1	-	45	60	60	Bath + Probe	20+20
Set 8	Span 60	0.5	0.1	0.13	45	60	60	Probe	20
Set 9	Tween60	0.1	0.05	-	45	-	-	-	-
Set 10	**Span60: Tween60**	**0.25: 0.25**	**0.1**	**0.13**	**45**	**60**	**60**	**Extru-sion**	**10 times**

Note: Conc: Concentration, mM: millimole, Chol: Cholesterol, Evapo.: Evaporation, min: Minutes, sonic: Sonication/Ultrasonication

The effect of these factors on the thin film, dispersion quality, and vesicle sizes after preparation and after storage of a week are summarized in Table 4.5.

Table 4.5. Effect of formulation and process variables on film, dispersion and vesicles

	After Preparation				After 7 days		
Parameter Sets	**Film Quality**	**Dispersion Quality**	**Av.Size, nm**	**PDI**	**Av.Size, nm**	**PDI**	**Appearance**
Set 1	Bad	-	-	-	-	-	-
Set 2	Good	good	881	0.70	927	0.8	Clump
Set 3	Good	good	525	0.65	2700	0.5	Clump
Set 4	Bad	-	-	-	-	-	-
Set 5	Good	bad	-	-	-	-	-
Set 6	Bad	-	-	-	-	-	-
Set 7	Good	good	612.8	0.6	742	1	Clump
Set 8	Good	good	519.4	0.65	1242	1	Clump
Set 9	Bad	-	-	-	-	-	-
Set 10	Good	good	185	0.4	221	0.4	Good

"-" indicates not measured or assessed because of poor quality film or dispersion,

Av.Size: Average Size

The formulation and process variable set 10 was considered the optimal since it resulted in the best combination of film, dispersion and vesicle size & stability.

4.3. Composition of the Optimized Formulations

From Table 4.4, the composition of the optimized formulation with methyl laurate and saw palmetto extract are shown in Table 4.6. Two similar formulations without edge-activator Na-cholate are also included for comparison purpose. They were all treated with the process conditions of set 10, that is, evaporation temperature of 45˚ C, hydration temperature of 60˚ C, and size reduction method of extrusion.

Table 4.6. Optimized formulations of ML and SPE niosomes

	Concentrations/Amounts	
Ingredients	**ML Niosomes**	**SPE Niosomes**
Span 60	0.25 mM	0.25 mM
Tween 60	0.25 mM	0.25 mM
Cholesterol	0.12 mM	0.12 mM
Sodium cholate	0.13 mM	0.13 mM
ML	10 mg	-
SPE	-	10 mg
PBS	q.s. 10 mL	q.s. 10 mL

ML Niosomes, SPE Niosomes are coded in the following as as MLnio, SPEnio, respectively.

4.4. Results of Characterization Studies on Optimized Formulations

4.4.1. Vesicle Size, PDI and Zeta-potential

The values of average vesicle size, zeta-potential as well as polydispersity index (PDI) are presented in Table 4.7.

Table 4.7. Size, PDI, and zeta potential of optimized formulations

Formulas	**Z-Average Size** ±SD**, nm**	**PDI**±SD	**Zeta-potential**±SD**, mV**
MLnio	185±0.778	0.44±0.008	-17.3±0.850
SPEnio	176±0.368	0.31±0.001	-17.8±0.451

Typical size distribution (by intensity) graphs of some vesicles are shown in Figure 4.5 and 4.6. They were typically multimodal after probe or bath sonication, but became unimodal after several extrusion through polycarbonate filter.

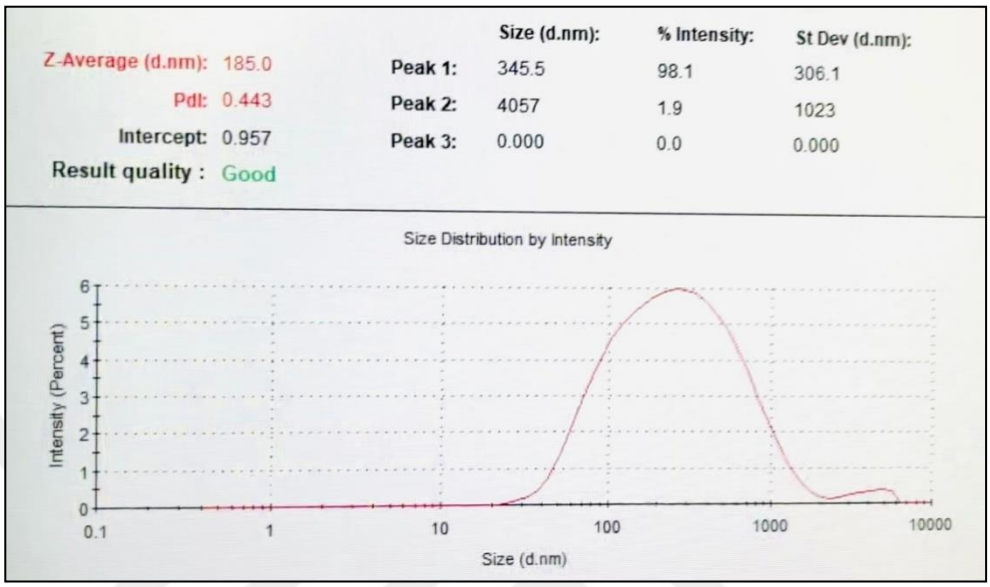

Figure 4.5. MLnio size distribution graph

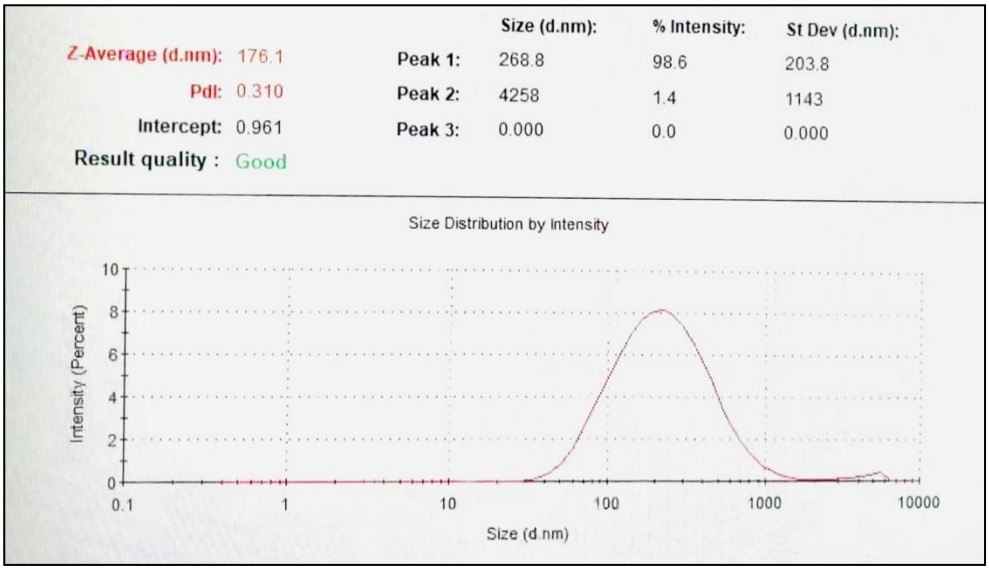

Figure 4.6. SPEnio size distribution graph

4.4.2. Vesicle Morphology by SEM

The electron photomicrographs of the optimized formulations are shown in the following Figures (Figure 4.7-4.8). The shapes of the niosomes were found to be spherical in general. Some were found to be shapless within the same formulation, for example. It is suspected that drying of the niosome samples (as required for electron microscopic investigation) might have affected the vesicle shapes. This suspicion is further strengthened by the irregularity/inward collapsing on the surfaces of some vesicle.

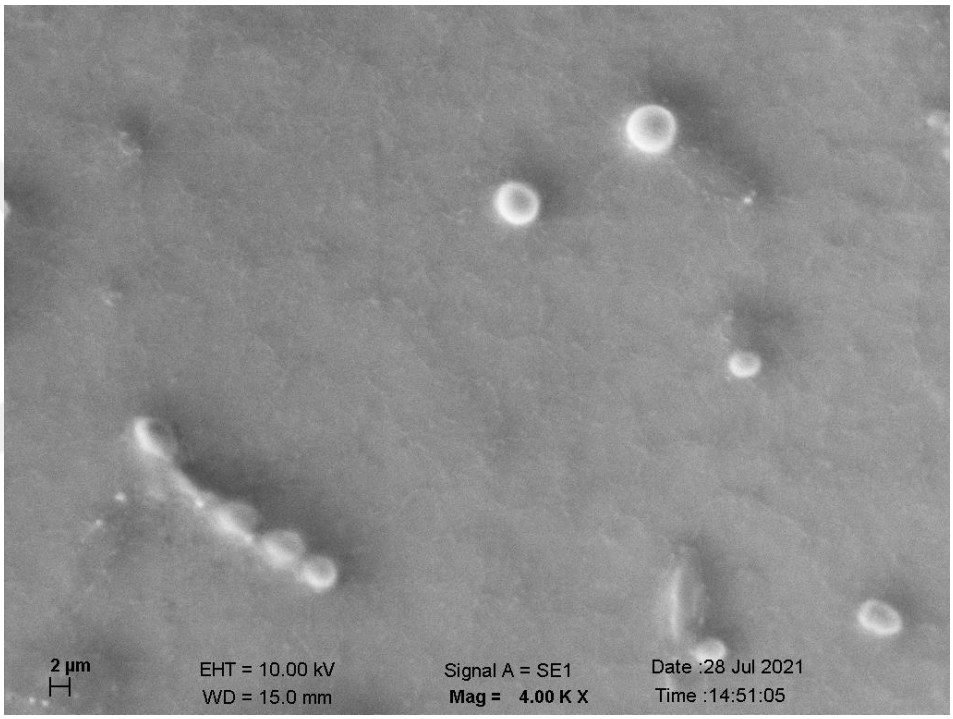

Figure 4.7. Electron photomicrograph of MLnio

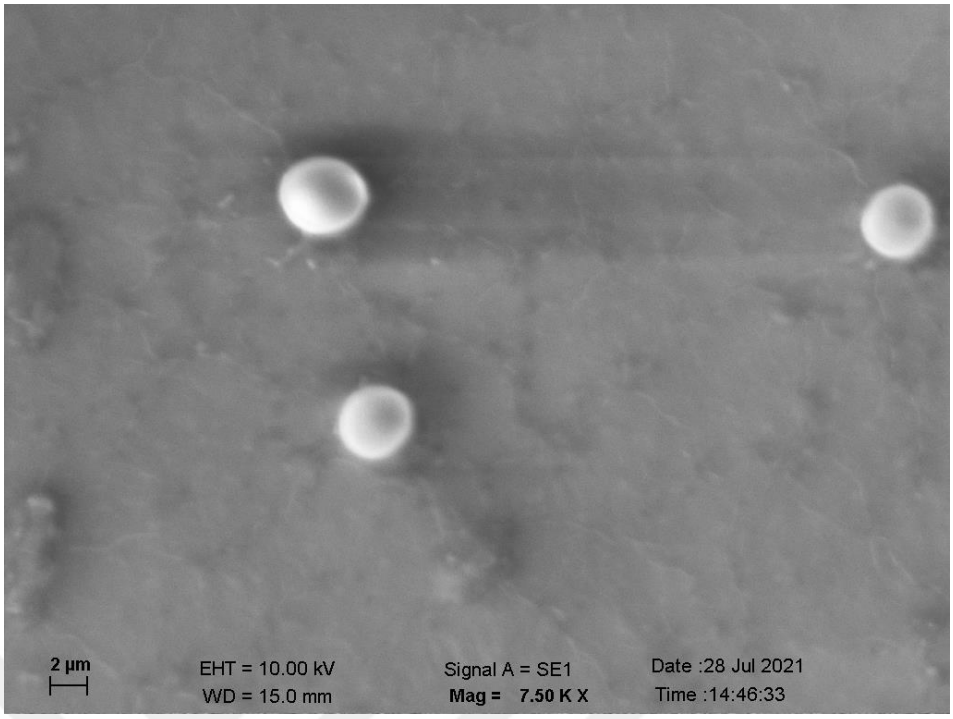

Figure 4.8. Electron photomicrograph of SPEnio

4.4.3. Qualitative Entrapment Capacity

Zero, 1, 2, 2.5, 4 mg of ML to 0.1 mM surfactant were tested. The maximum amount of ML that could be incorporated with 0.1 mM of surfactant was 2 mg. This amount produced smooth flawless film as shown in Figure 4.9, as well as homogenous dispersion after hydration with no observed ML droplets under microscope as shown in Figure 4.11. On the other hand, the addition of further amount of ML formed a film with yellowish oily spots belonging to ML as seen in Figure 4.10., as well as obvious entrapped drops observed under light microscope as shown in Figure 4.12.

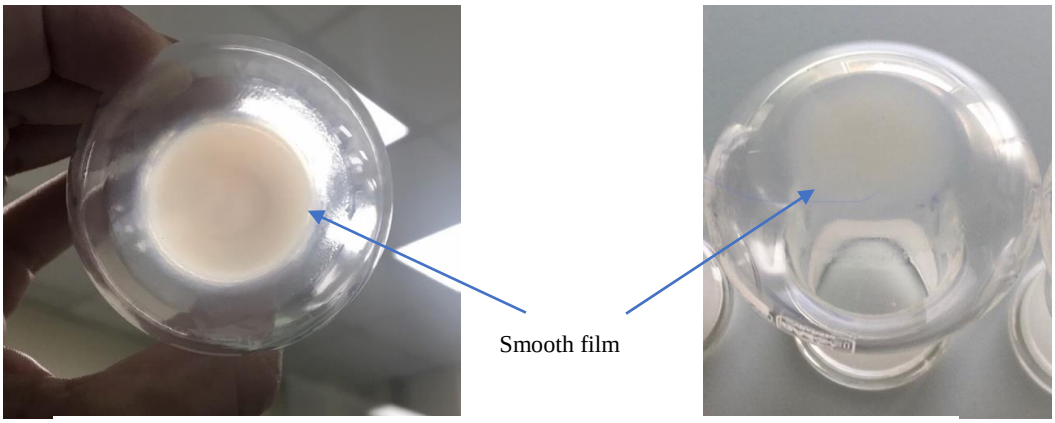

Figure 4.9. Smooth and homogenous film showing no unentrapped ML spots

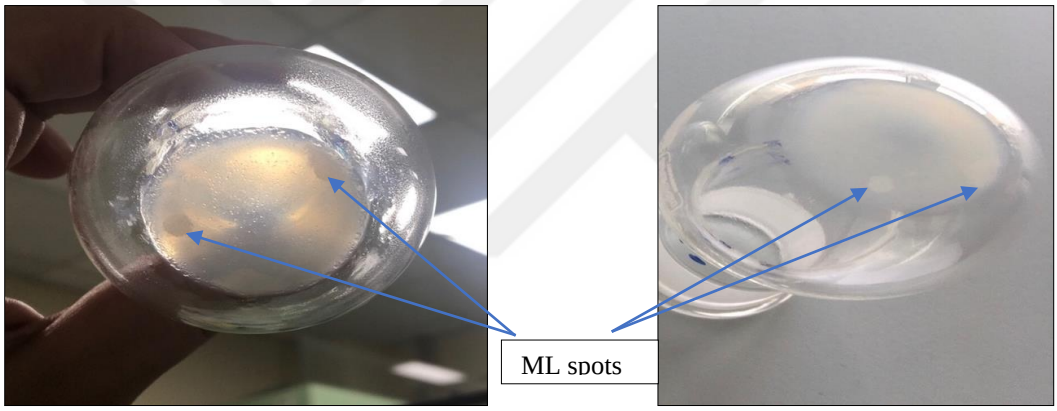

Figure 4.10. Thin film showing unentrapped ML spots

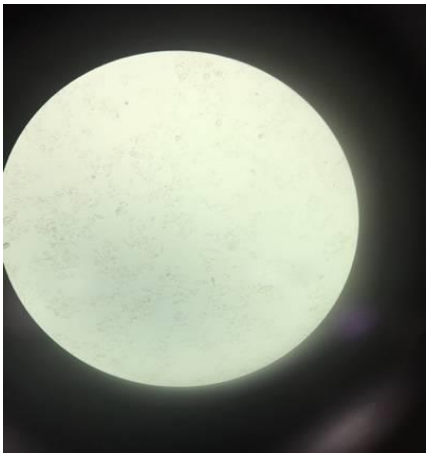

Figure 4.11. Light microscope picture showing homogenous ML dispersion with no ML droplet

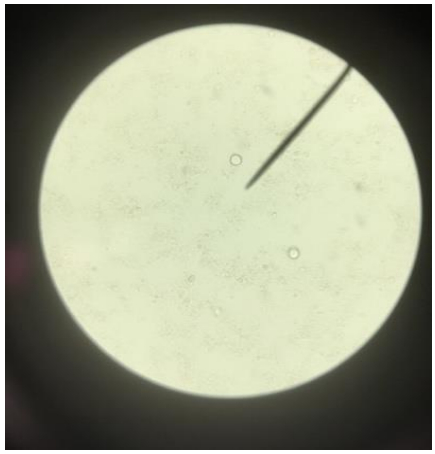

Figure 4.12. Light microscope picture showing unentrapped ML droplets

The same observations were found with SPE formulations as shown in Figures 4.13 – 4.16.

Figure 4.13. Smooth and homogenous SPE film showing no unentrapped SPE spot

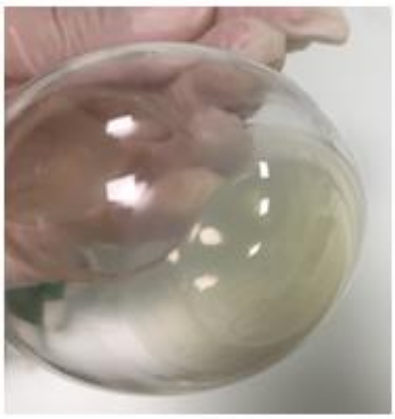

Figure 4.14. Thin film showing huge unentrapped SPE spot (circle)

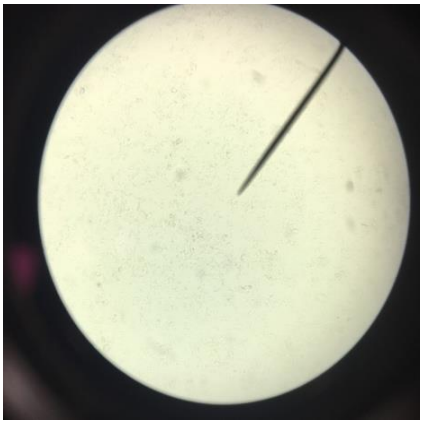

Figure 4.15. Light microscope picture showing homogenous vesicles with no unentrapped SPE droplet

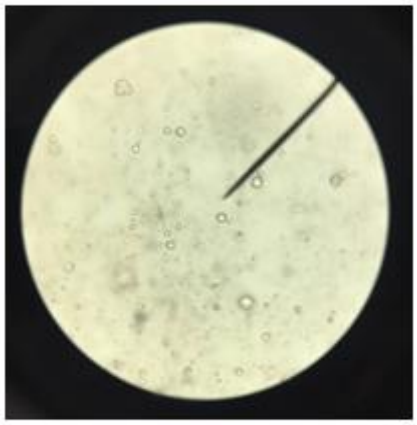

Figure 4.16. Light microscope picture showing unentrapped SPE droplets

4.4.4. Elasticity/Deformability

As mentioned before, niosomes consisting of Span 60 as the only surfactant could not be extruded through polycarbonate filters. This meant they were the most inelastic or rigid vesicles. Calculated by the method as explained in section 3.2.5, deformabilities of the optimized formulations are given in Table 4.8 below.

Table 4.8. Deformability index values of niosome formulations

Niosomes	**Deformability Index**
MLnio	0.89
SPEnio	1.06

4.4.5. Stability

Initial study results are shown in Table 4.9. There was moderate increase in vesicle size at both temperatures but significant increase in PDI for the samples kept at room temperature, while the one at 4˚ C retained its PDI. Room temperature sample

showed phase separation. This study indicated that niosome needs to be either stored in refrigerator or formulated in enmeshing polymer structure like gels.

Table 4.9. Size and PDI of niosomes stored at 4˚ C and 25˚ C after 7 days

Temperature˚ C	**Average Size, nm**	**PDI**
4-8	221.9	0.5
25	280.2	0.8

The stability results for both ML and SPE optimized formulations after 1, 2, and 4 months are shown in Table 4.10.

Table 4.10. Stability results for ML and SPE optimized formulations at 4-8˚C

Time, months	**Parameter**	**MLnio**	**SPEnio**
1	Mean Size, nm	241.0	278.0
	PDI	0.8	0.9
2	Mean Size, nm	198.2	200.8
	PDI	0.6	0.6
4	Mean Size, nm	402.8	336.9
	PDI	0.6	0.9

4.4.6. Permeability Study

The amount of ML found in each donor compartment after 6 h and the corresponding flux and permeability are shown in Table 4.11. This study was performed for the comparison of different membranes.

Table 4.11. Flux and permeability of ML through different membranes

Membranes	Conc (mg/mL)	Flux (mg/cm^2/hr)	Permeability (cm/hr)
Strat M	0.08	0.05	0.02
0.45 filter	0.20	0.14	0.05

The results of multipoint permeability studies done with StratM membrane are presented in Table 4.12 below.

Table 4.12. Flux and permeability rate for methyl laurate from MLnio niosome

Time (hr)	Result conc. (mg/mL)	Flux (mg/cm^2/hr)	Permeability (cm/hr)	Cumulative amount permeated/cm (mg)
2	0.003	0.002	0.00007	0.02
4	0.010	0.007	0.00200	0.07
6	0.020	0.010	0.00500	0.17
8	0.030	0.020	0.00700	0.32

Permeation profile for ML through Strat-M membrane is presented in Figure 4.17.

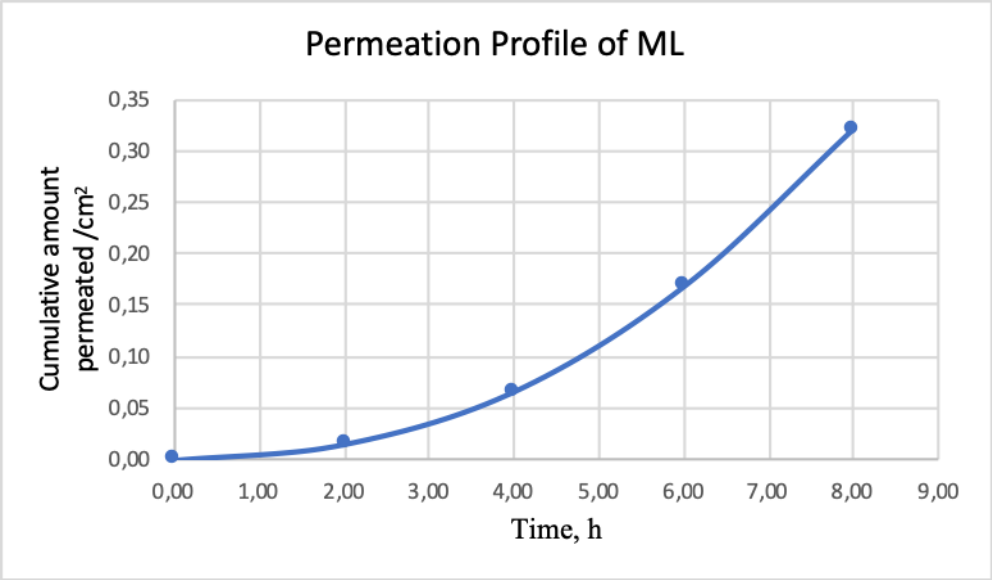

Figure 4.17. Permeation profile for ML through Strat-M membrane

The steady state flux is represented by the slope of the linear part (R^2 = 0.9868) of the graph as shown in Figure 4.18. It is found to be 0.0638 (mg/cm^2/hr) and the corresponding permeability coefficient is 0.06 cm/hr.

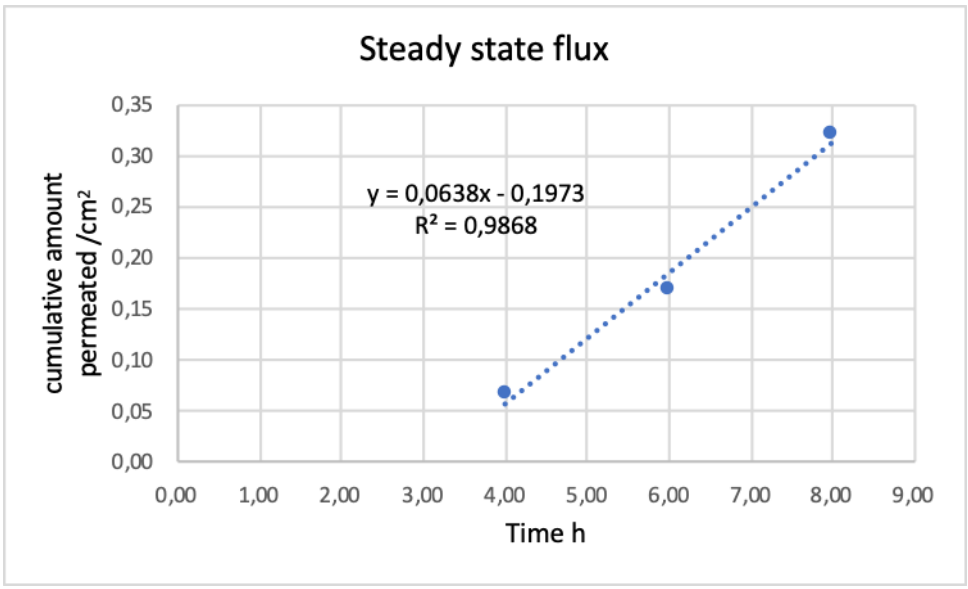

Figure 4.18. Linear part of permeation profile

4.5. Evaluation of Gel Preparations

4.5.1. Density and pH Values for Gel Preparations

As explained in 3.2.6, four different gel formulations were prepared. Their densities and pH values are given in Table 4.13.

Table 4.13. Density and pH of gel preparations

Preparations	Density (g/mL)	pH
MLnioG	0.949	6.07
SPEnioG	0.979	6.05
BLANKnioG	0.954	6.05
BLANKG	1.025	6.09

4.5.2. Shear Rate, Viscosity and Shear Stress Data for Gel Preparations

The viscosity, shear rate and shear stress data for these preparations are reported in Table 4.14 – 4.17., and their corresponding rheograms are presented in Figure 4.19 – 4.22.

Table 4.14. Viscosity data for BLANKG

Shear rate (cm^{-1})	Viscosity (cP)	Shear stress ($dyne/cm^2$)
1	5000	50.0
2	4375	87.5
5	3050	152.5
10	2250	225.0
20	1650	327.5
30	1358	405.0
40	1181	472.5
50	1060	532.0

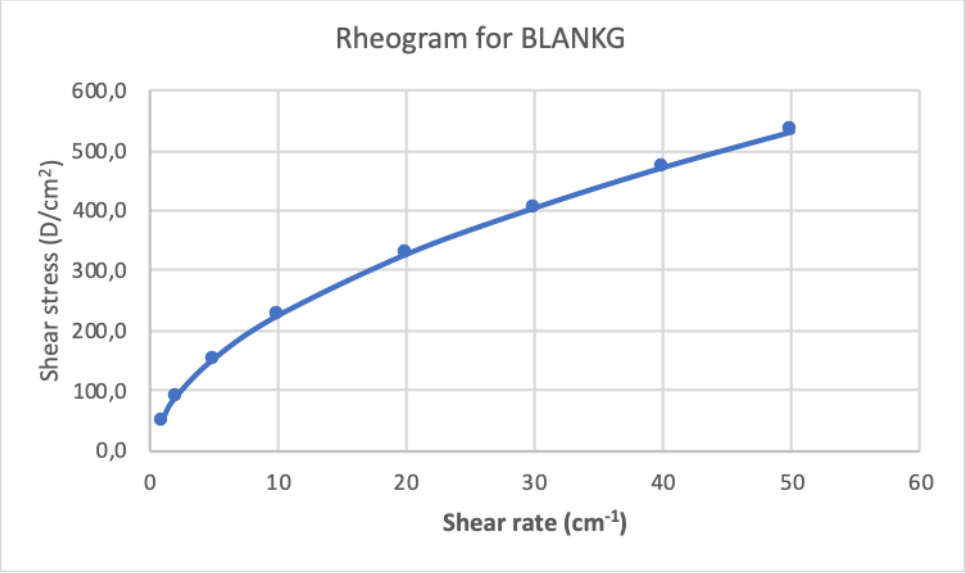

Figure 4.19. Rheogram of CMC-Na blank gel containing no niosomes (BLANKG)

Table 4.15. Viscosity data for BLANKnioG

Shear rate (cm^{-1})	Viscosity (cP)	Shear stress ($dyne/cm^2$)
1	8750	87.5
2	6500	130.0
5	4250	212.5
10	3225	322.5
20	2238	447.5
30	1825	547.5
40	1581	630.0
50	1405	702.0

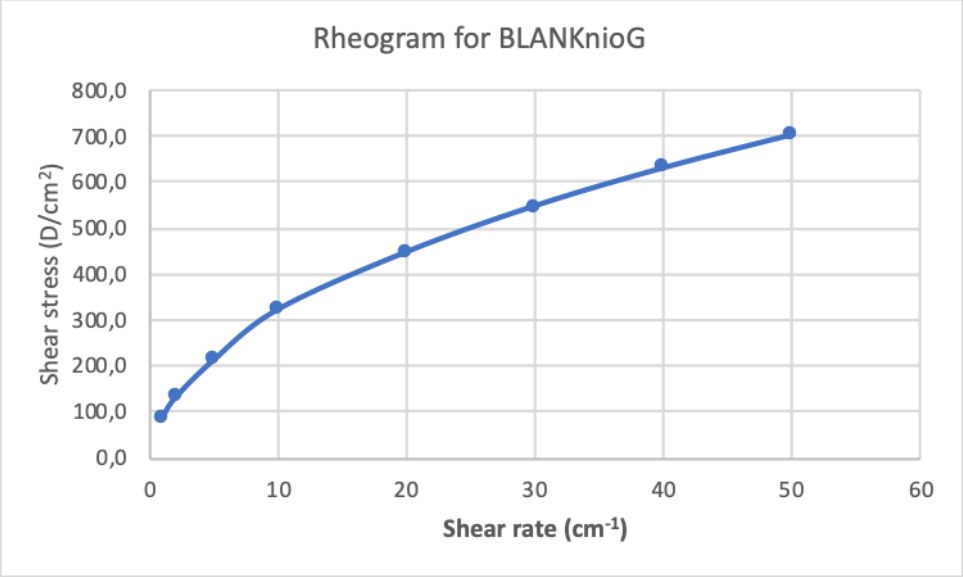

Figure 4.20. Rheogram of CMC-Na Gel incorporating blank (empty) niosome

Table 4.16. Viscosity data for MLnioG

Shear rate (cm^{-1})	Viscosity (cP)	Shear stress ($dyne/cm^2$)
1	7750	77.5
2	6000	120.5
5	4250	212.0
10	3075	307.0
20	2163	432.5
30	1750	525.0
40	1449	579.0
50	1380	697.0

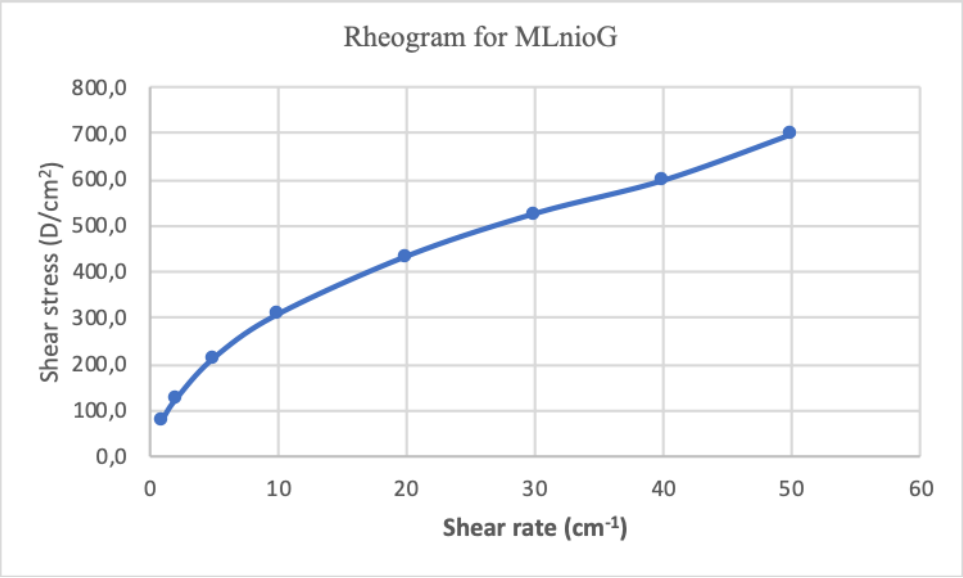

Figure 4.21. Rheogram of CMC-Na Gel incorporating ML niosome

Table 4.17. Viscosity data for SPEnioG

Shear rate (cm^{-1})	Viscosity (cP)	Shear stress ($dyne/cm^2$)
1	7500	75.0
2	6000	120.0
5	4100	205.5
10	3075	307.5
20	2150	430.5
30	1775	532.5
40	1525	607.5
50	1360	682.5

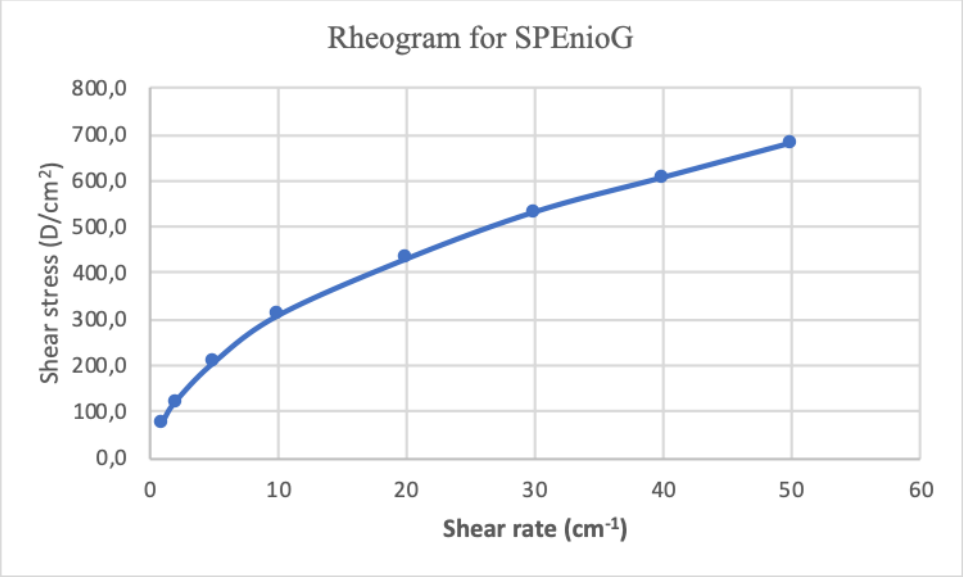

Figure 4.22. Rheogram of CMC-Na Gel incorporating SPE niosome

4.5.3. Shear stress - Shear rate Correlation and Plastic Viscosity

The correlation between shear stress and shear rate in the linear portion of the rheograms are shown in Figure 4.23-4.26. Plastic viscosities are expressed as the slope of these linear portions. These are summarized in Table 4.18.

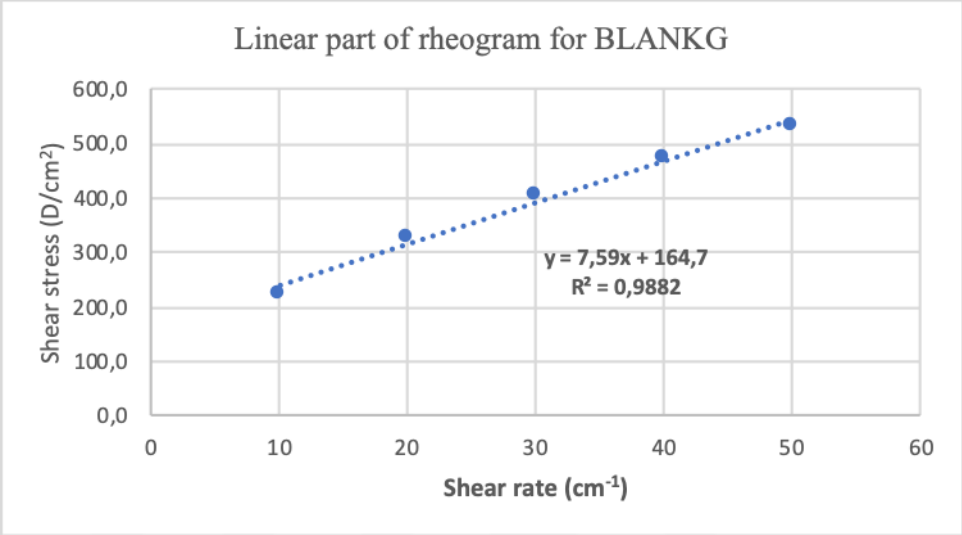

Figure 4.23. Shear stress vs shear rate correlation of linear part of rheogram BLANKG

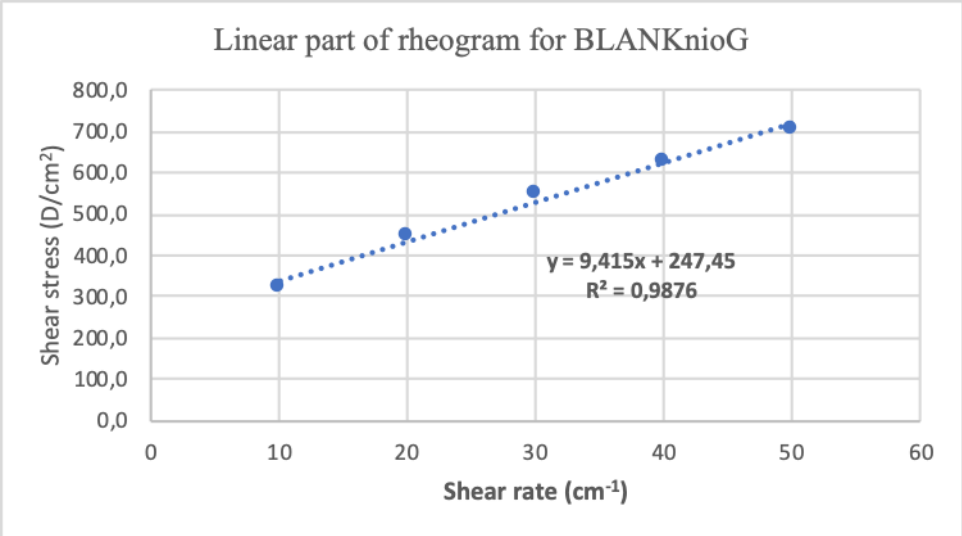

Figure 4.24. Shear stress vs shear rate correlation of linear part of rheogram BLANKnioG

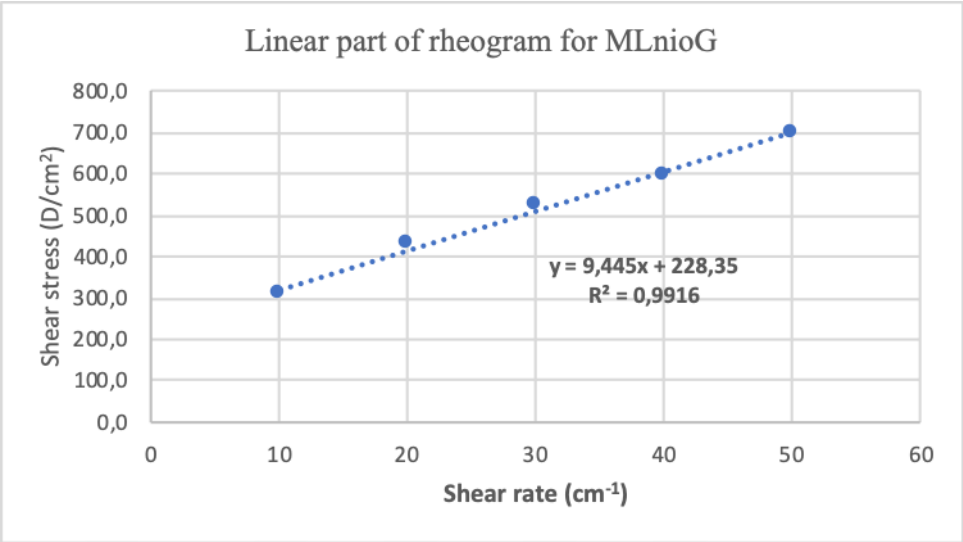

Figure 4.25. Shear stress vs shear rate correlation of linear part of rheogram MLnioG

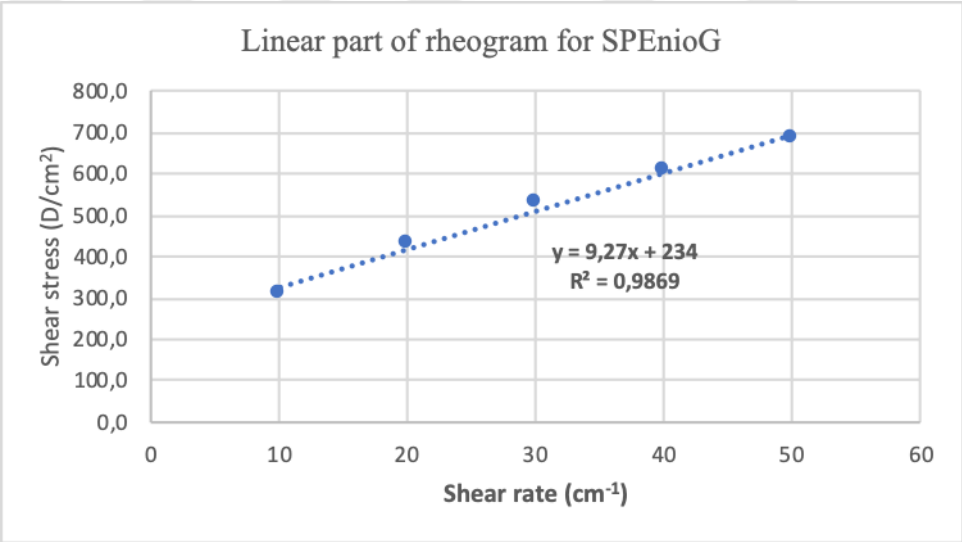

Figure 4.26. Shear stress vs shear rate correlation of linear part of rheogram SPEnioG

Table 4.18. Shear rate-shear stress correlation and plastic viscosities

Niosome-Gel Formulations	Shear rate-Shear stress correlation	Plastic Viscosities
BLANKG	0.9882	7.59
BLANKnioG	0.9876	9.41
MLnioG	0.9916	9.44
SPEnioG	0.9869	9.27

5. DISCUSSION AND CONCLUSION

5.1. Discussion

The purpose of this study was to formulate, prepare and characterize niosomes carrying anti-alopecia active ingredient (*Serenoa repens* extract), and its component *Methyl Laurate*, and incorporate them into gel preparations to enhance their shelf stability and ease of application onto the scalp for the treatment of AGA. Androgenic Alopecia (AGA), is mainly caused by dihydrotestosterone which is mediated by 5-alpha reductase enzyme (1), micro inflammation, insulin resistance, and other factors. The management of AGA with topical treatments present in the market is doubtful and not sufficient, comprising many unwanted side effects (2).

Saw Palmetto extract has shown significant inhibitory activity in in vitro test against 5-alpha reductase enzyme (11-15) due to the presence of several active fatty acids (19) and sterols (2). It has also shown some topical activity (17-18) which can be improved by incorporating it into a skin penetrating carrier vesicle. Niosomes, for example, are promising transdermal penetrating bilayer vesicles (9) with size ranging between 20 and 1000 nm, making them perfect for hair follicle penetration (10).

Niosomes are non-ionic surfactant vesicles which can be used as carriers for hydrophilic and lipophilic drugs (7-8). Their small size and the addition of edge activator such as sodium cholate makes them elastic (48-49) and suitable to penetrate and accumulate in hair follicles (53) making them great carriers for anti-alopecia treatment.

Because the vesicular dispersion has low viscosity and tends to sediment over time, incorporating them into gel preparation is advantageous to increase the formulation stability and to make the application to the scalp easier. For this reason, vesicular emulsions were incorporated into CMC-Na gel preparations which are simple preparations with few ingredients easily forming a gel with favorable qualities.

One of the most repeatedly used buffer solutions is Phosphate Buffered Saline, a physiologically relevant salt solution composed of Sodium monophosphate Potassium diphosphate Sodium chloride Potassium chloride. It was prepared using ultra purified water and the pH was adjusted to 5.5 using 5 % HCL to accord with the natural pH of the scalp.

In accordance with HPLC methods developed by Guarrasi et al. (78) Methyl Laurate was tested at 208 nm and the retention time was found to be 3.5 ± 0.1 minutes. A 6-point calibration curve was prepared using 1, 0.5, 0.25, 0.1, 0.05, 0.02 mg/mL of ML in mobile phase with 3 replicates for each point. The correlation was clearly linear as seen in Figure 4.3 with correlation coefficient R= 0.9975. The intra-assay accuracy, the proximity of measured concentration to added concentration, ranged between -2.28 and 6 % at three concentrations 0.75, 0.4, 0.075 mg/mL level, for which the precision, the proximity to average, ranged between 6.38 and 10.89 %. The inter-assay accuracy for the same concentrations ranged between 6.67 and 11.75 % whilst the precision, the proximity to average, ranged between 9.82 and 11.91 % as seen in Figure 4.4 the inter-assay precision values are almost inextricable for each concentration level.

Niosomes composed of surfactant, cholesterol, Na cholate, and either ML or SPE were prepared by Thin Film (hand shaking) method. First, initial studies were performed by manipulating different parameters in order to get the best formulation referred to as the "optimized formulation". These parameters are surfactant type, Cholesterol to surfactant ratio, Surfactant to ML concentration ratio, evaporation temperature, rotation speed, hydration method, temperature and time, and size reduction method. As a result, it was found that 0.1 mM surfactant was able to load nearly 100% of 2 mg active ingredient in the presence of cholesterol or cholesterol- Na cholate mixture in a ratio 1:5 to surfactant.

In the preparation of the optimized formulations by thin film method, all the ingredients were dissolved in chloroform/ methanol mixture which was then completely evaporated at 45˚ C in a rotary evaporator. Any residual solvent was removed from the film by desiccator overnight before film hydration by PBS pH 5.5 at 60˚C using magnetic stirrer. Size reduction was performed by extrusion through a 400 nm filter at 40˚C extruder. Later on, size measurement was performed using DLS zetasizer, where size of ML and SPE niosomes was found 185 nm and 176 nm respectively, with PDI 0.4 and 0.3 respectively. This size range is suitable for hair follicle penetration and accumulation as explained in section 2.4.1 E.

Because of the oily nature of ML and SPE, we reasoned that the conventional method of the determination of entrapment efficiency is not suitable since the oily material will tend to remain with the surfactant vesicles rather than in the aqueous

supernatant after centrifugation. Thus, a much simpler method, spotting, was employed to approximately determine the amount that is most likely to be incorporated within the niosome. The addition of more than 2 mg ML or SPE per 0.1 mM surfactant caused the appearance of clear oily spots in the thin film. Though this is not a quantitative one, we put forward this as an applicable method for working with materials of similar density, which are extremely difficult to separate, especially if intended preparation is topical.

Other characterizations such as deformability and dispersion stability tests were implemented. Deformability, the measurement of elasticity, for MLnio and SPEnio were measured by extrusion and were found to be 0.89 and 1.06 respectively. Emulsion stability was determined by the physical appearance of dispersion (separation or presence of chunks), size measurement, and PDI measurement. Initial study's preparations after 7 days showed various changes in vesicle size and appearance with occurrence of sedimentation in some of them, but formula 10, later referred as optimized formulation, showed the most favorable characteristics with minimal changes. Optimized formulations after storage for 10 days at 4˚C showed better qualities than at room temperature, that's why the next stability test was performed at 4˚C after 1, 2, and 4 months showing slight increase in size but substantial increase in PDI.

Permeability, the flow rate of material through porous membrane, was tested by Franz Cell diffusion apparatus for ML niosome formulation since ML was taken as a representative for SPE. Since there are only few studies on our target membrane Strat-M we decided to perform a quick comparison study between Strat-M and 0.45 µm nylon filter. The results after 6 hours (Table 4.11.) showed maximum permeability 0.05 cm/hr through 0.45 µm filter with flux 0.14 mg/cm^2/hr and minimum permeability 0.02 cm/hr through Strat-M membrane with flux 0.05 mg/cm^2/hr. We are not sure about whether the permeation mode is molecular or vesicular. Because ML is not soluble in the buffer, the most logical guessing is vesicle being transported. These elastic vesicles are supposed to penetrate through very narrow pores, the size of which can be a fraction of their own sizes.

The permeability study through human skin alternative Strat-M membrane over a period of 8 hours shown in Table 4.12., revealed a flux ranging between 0.02 and 0.002 (mg/cm^2/hr) with (P=0.0087), permeability ranging between 0.002 and 0.00007

(cm/hr) with (P=0.0075), and cumulative permeability ranging between 0.02 and 0.32 (mg/cm^2) with (P=0.0007). The steady state flux (*Jss*) was calculated from the slope of the linear part of the permeability profile and was found equal to 0.0638 (mg/cm^2/hr) with a corresponding permeability constant of 0.06 cm/hr according to *Fick's Law*.

Gel is a good dosage form to be applied to the scalp. We found it the most suitable carrier for our niosome formulation. Four gel preparations were prepared by stirring the gelling agent CMC-Na and preservatives (Methyl and Propyl paraben) in PBS pH 5.5 using a magnetic stirrer with addition of glycerin as a humectant. As soon as the gels are formed, one was left as it is for comparison purpose while empty niosome, ML loaded niosome, and SPE loaded niosome were added to the remaining three in a concentration 20 % w/w. The addition of niosome to the gel caused a very slight decrease in density which is understandable due to the oily nature of the niosome. The pH of all gel preparations was around 6 which is pretty much acceptable for scalp application.

Tables 4.13–4.16 and their corresponding Figures 4.19–4.21 display the viscosity, shear rate and shear stress data of the four gel preparations. As noticed from the data, the addition of niosome caused a slight increase in the viscosity of the gel. For example, the viscosity of the blank gel at shear rate 1 cm^{-1} was 5000 cP while for other gel preparations it ranged between 7500 and 8750 cP. Same for the shear stress which increased from 50 (dune/cm^2) for the blank gel to the range of 75 to 87.5 for the other gels at shear rate 1 cm^{-1}.

The correlation coefficients (R^2) of linear portion for rheograms BLANKG, BLANKnioG, MLnioG, and SPEnioG shown in Figures 4.23–4.26 are 0.99, 0.99, 0.92, and 0.99 respectively, which confirms linearity. The plastic viscosities of these gels, expressed as the slope of the linear portion for rheograms, are 7.59, 9.42, 9.45, 9.27 cP respectively, which confirms that the addition of niosome increases the gel viscosity slightly, however this increase is hardly noticeable when the gel was practically applied to the skin.

5.2. Conclusion

In conclusion, the surfactant vesicles, niosomes, are appropriate delivery carriers for active substances, like anti alopecia agents, deeper into the hair follicle. Numerous

active substances, either hydrophilic or lipophilic, can be loaded into these vesicles at the same time. However, their sizes must be less than 600 nm considering the sizes of hair follicle orifice. CMC-Na gels are a decent carrier for Niosome. These gel formulations with incorporated Niosomes provided convenient consistency for topical application to the scalp.

6. REFERENCES

1. Wolff K, Johnson R., Saavedra AP. Disorders of Hair Follicles and Related Disorders. In: McGraw-Hill Education, ed. *Fitzpatrick Color Atlas and Synopsis of Clinical Dermatology*. 8th ed; 2013:760-784.

2. Sadgrove NJ. The new paradigm for androgenetic alopecia and plant-based folk remedies: 5α-reductase inhibition, reversal of secondary microinflammation and improving insulin resistance. *J Ethnopharmacol*. 2018;227:206-236.

3. Jadhav SM, Morey P, Karpe MM, Kadam V. Novel vesicular system: An overview. *J Appl Pharm Sci*. 2012;2(1):193-202.

4. Ascenso A, Raposo S, Batista C, et al. Development, characterization, and skin delivery studies of related ultradeformable vesicles: Transfersomes, ethosomes, and transethosomes. *Int J Nanomedicine*. 2015;10:5837-5851.

5. Sala M, Diab R, Elaissari A, Fessi H. Lipid nanocarriers as skin drug delivery systems: Properties, mechanisms of skin interactions and medical applications. *Int J Pharm*. 2018;535(1-2):1-17.

6. Jain S, Jain V, Mahajan SC. Lipid Based Vesicular Drug Delivery Systems. *Adv Pharm*. 2014;2014:1-12.

7. Helal DA, Teaima MH, El-Rhman DA, Abdel-Halim SA, El-Nabarawi M. Preparation and Evaluation of Niosomes Containing an Anticellulite Drug. *Inven Impact Pharma Tech*. 2015;2(3):95-101.

8. Bini KB, Akhilesh D, Prabhakara P, Kamath J V. Development and characterization of non-ionic surfactant vesicles (niosomes) for oral delivery of lornoxicam. *Int J Drug Dev Res*. 2012;4(3):147-154.

9. Md. Rageeb Md. Usman PRG, Jain B V. Niosomes : A Novel Trend of Drug Delivery of Biomedical. *Eur J Biomed Pharm Sci*. 2017;4(7):436-442.

10. Nohynek GJ, Lademann J, Ribaud C, Roberts MS. Grey Goo on the skin? Nanotechnology, cosmetic and sunscreen safety. *Crit Rev Toxicol*. 2007;37(3):251-277.

11. Sultan C, Terraza A, Devillier C, et al. Inhibition of androgen metabolism and binding by a liposterolic extract of “serenoa repens B” in human foreskin fibroblasts. *J Steroid Biochem*. 1984;20(1):515-519.

12. Iehlé C, Délos S, Guirou O, Tate R, Raynaud J, Martin P. Human prostatic steroid 5 alpha-reductase isoforms--a comparative study of selective inhibitors. *J Steroid Biochem Mol Biol*. 54(5/6):273-279.

13. Habib FK, Ross M, Ho CKH, Lyons V, Chapman K. Serenoa repens (Permixon®) inhibits the 5α-reductase activity of human prostate cancer cell lines without interfering with PSA expression. *Int J Cancer*. 2005;114(2):190-194.

14. Pais P, Villar A, Rull S. Determination of the potency of a novel saw palmetto supercritical CO2 extract (SPSE) for 5α-reductase isoform II inhibition using a cell-free in vitro test system. *Res Reports Urol*. 2016;8:41-49.

15. Pais P. Potency of a novel saw palmetto ethanol extract, SPET-085, for inhibition of 5α-reductase II. *Adv Ther*. 2010;27(8):555-563.

16. Prager N, Bickett K, French N, Marcovici G. A randomized, double-blind, placebo-controlled trial to determine the effectiveness of botanically derived inhibitors of 5-α-reductase in the treatment of androgenetic alopecia. *J Altern Complement Med*. 2002;8(2):143-152.

17. Arca E, Açıkgöz G, Yeniay Y, Çalışkan E. The Evaluation of Efficacy and Safety of Topical Saw Palmetto and Trichogen Veg Complex for the Treatment of Androgenetic Alopecia in Men. *Turkish J Dermatology / Türk Dermatoloji Derg*. 2014;8(4):210-215.

18. Wessagowit V, Tangjaturonrusamee C, Kootiratrakarn T, et al. Treatment of male androgenetic alopecia with topical products containing Serenoa repens extract. *Australas J Dermatol*. 2016;57(3):e76-e82.

19. Abe M, Ito Y, Suzuki A, Onoue S, Noguchi H, Yamada S. Isolation and pharmacological characterization of fatty acids from saw palmetto extract. *Anal Sci*. 2009;25(4):553-557.

20. Mescher AL. Junqueira’s Basic Histology: Text and Atlas. In: 15th ed. McGraw Hill Education; 2018:14/26-16/26.

21. Jain PK, Joshi H, Dass DJ. Drug that Causes Hair Loss and Promotes Hair Growth - A Review. *Int J Res Pharm Biomed Sci*. 2012;3(4):1476-1482.

22. Bandaranayake I, Mirmirani P. Hair loss remedies - Separating fact from fiction. *Cutis*. 2004;73(2):107-114.

23. Bolognia JL, Braverman IM. Skin Manifestations of Internal Disease. In: Jameson JL, Fauci AS, Kasper DL, Hauser SL, Longo DL, Loscalzo J, eds. *Harrison's Principles of Internal Medicine*. 20th ed. McGraw-Hill Education; 2018.

24. Rutter P, Community pharmacy: symptoms, diagnosis and treatment. Elsevier Health Sciences; 2020 May 27.

25. Thomas J. *The Alopecias*. 1st ed. Jaypee Brothers, Medical Publishers Pvt. Limited; 2018.

26. Hordinsky MK. Hair Disorders. In: *Clinical Dermatology*. 1st ed. McGraw-Hill Education;2013. Chapter 19

27. Regional Interpretation - Other (California and Florida) | NRCS. Published 2018. Available from https://www.nrcs.usda.gov/wps/portal/nrcs/detail/national/technical/nra/nri/results/?cid=nrcseprd1343040. Access 25/05/2021

28. Deelen V, Timothy R. Serenoa repens. Fire Effects Information System. Published 1991. Available from https://www.fs.fed.us/database/feis/plants/shrub/serrep/all.html. Accessed 11/03/2020

29. Murugusundram S. Serenoa repens: Does it have any role in the management of androgenetic alopecia? *J Cutan Aesthet Surg*. 2009;2(1):31. doi:10.4103/0974-2077.53097

30. Penugonda K, Lindshield BL. Fatty acid and phytosterol content of commercial saw palmetto supplements. *Nutrients*. 2013;5(9):3617-3633.

31. Leaflet I. *INFORMATION LEAFLET Ph . Eur . Reference Standard*. Vol 33.; 2016.

32. Shi R, Xie Q, Gang X, et al. Effect of saw palmetto soft gel capsule on lower urinary tract symptoms associated with benign prostatic hyperplasia: A randomized trial in Shanghai, China. *J Urol*. 2008;179(2):610-615.

33. Gerber GS, Kuznetsov D, Johnson BC, Burstein JD. Randomized, double-blind, placebo-controlled trial of saw palmetto in men with lower urinary tract symptoms. *Urology*. 2001;58(6):960-963.

34. Goldmann WH, Sharma AL, Currier SJ, Johnston PD, Rana A, Pal Sharma C. Saw Palmetto berry extract inhibits cell growth and Cox-2 expression in prostatic cancer cells. *Cell Biol Int*. 2001;25(11):1117-1124.

35. Yang Y, Ikezoe T, Zheng Z, Taguchi H, Koeffler HP, Zhu WG. Saw Palmetto induces growth arrest and apoptosis of androgen-dependent prostate cancer LNCaP cells via inactivation of STAT 3 and androgen receptor signaling. *Int J Oncol*. 2007;31(3):593-600.

36. Raynaud JP, Cousse H, Martin PM. Inhibition of type 1 and type 2 5α-reductase activity by free fatty acids, active ingredients of Permixon®. *J Steroid Biochem Mol Biol*. 2002;82(2-3):233-239.

37. Goldberg EP. Liposome Technology. In: Poste G, Krisch R, Koestler T, eds. *Targeted Drugs*. Vol 3. John Wiley & Sons; 1983.

38. Bansal S, Kashyap CP, Aggarwal G, Harikumar SL. A comparative review on vesicular drug delivery system and stability issues. *Int J Res Pharm Chem*. 2012;2(3):704-713.

39. Vora B, Khopade AJ, Jain NK. Proniosome based transdermal delivery of levonorgestrel for effective contraception. *J Control Release*. 1998;54(2):149-165.

40. Shatalebi MA, Mostafavi SA, Moghaddas A. Niosome as a drug carrier for topical delivery of N-acetyl glucosamine. *Res Pharm Sci*. 2010;5(2):107-117.

41. Homaei M. Preparation and characterization of giant niosomes. Published online 2016.

42. Moghassemi S, Hadjizadeh A. Nano-niosomes as nanoscale drug delivery systems: An illustrated review. *J Control Release*. 2014;185(1):22-36.

43. Kumar GP, Rao PR. Ultra deformable niosomes for improved transdermal drug delivery: The future scenario. *Asian J Pharm Sci*. 2012;7(2):96-109.

44. Dayan N, Touitou E. Carriers for skin delivery of trihexyphenidyl HCl: Ethosomes vs. liposomes. *Biomaterials*. 2000;21(18):1879-1885.

45. Dragicevic-Curic N, Scheglmann D, Albrecht V, Fahr A. Temoporfin-loaded invasomes: Development, characterization and in vitro skin penetration studies. *J Control Release*. 2008;127(1):59-69.

46. El Maghraby GMM, Williams AC, Barry BW. Interactions of surfactants (edge activators) and skin penetration enhancers with liposomes. *Int J Pharm*. 2004;276(1-2):143-161.

47. Manconi M, Mura S, Sinico C, Fadda AM, Vila AO, Molina F. Development and characterization of liposomes containing glycols as carriers for diclofenac. *Colloids Surfaces A Physicochem Eng Asp*. 2009;342(1-3):53-58. doi:10.1016/j.colsurfa.2009.04.006

48. Trotta M, Peira E, Debernardi F, Gallarate M. Elastic liposomes for skin delivery of dipotassium glycyrrhizinate. *Int J Pharm*. 2002;241(2):319-327.

49. Cevc G. Transfersomes, liposomes and other lipid suspensions on the skin: Permeation enhancement, vesicle penetration, and transdermal drug delivery. *Crit Rev Ther Drug Carrier Syst*. 1996;13(3-4):257-388.

50. Lademann J, Weigmann HJ, Rickmeyer C, et al. Penetration of titanium dioxide microparticles in a sunscreen formulation into the horny layer and the follicular orifice. *Skin Pharmacol Appl Skin Physiol*. 1999;12(5):247-256.

51. Lademann J, Otberg N, Richter H, et al. Investigation of follicular penetration of topically applied substances. *Skin Pharmacol Appl Skin Physiol*. 2001;14(SUPPL. 1):17-22.

52. Schaffer M, Plewing G. Structure and Function of Eccrine, Apocrine and Sebaceous Glands. In: Bolognia J, Schaffer J, Cerroni L, eds. *Dermatology*. 4th ed. Elsevier; 2018:539-544.

53. Toll R, Jacobi U, Richter H, Lademann J, Schaefer H, Blume-Peytavi U. Penetration profile of microspheres in follicular targeting of terminal hair follicles. *J Invest Dermatol*. 2004;123(1):168-176.

54. Teichmann A, Ossadnik M, Richter H, Sterry W, Lademann J. Semiquantitative determination of the penetration of a fluorescent hydrogel formulation into the hair follicle with and without follicular closure by microparticles by means of differential stripping. *Skin Pharmacol Physiol*. 2006;19(2):101-105.

55. Lademann J, Richter H, Schaefer UF, et al. Hair follicles - A long-term reservoir for drug delivery. *Skin Pharmacol Physiol*. 2006;19(4):232-236.

56. Chen S, Hanning S, Falconer J, Locke M, Wen J. Recent advances in non-ionic surfactant vesicles (niosomes): Fabrication, characterization, pharmaceutical and cosmetic applications. *Eur J Pharm Biopharm*. 2019;144:18-39.

57. Billerit C. Methods Development For Biomembrane Model Systems. Published online 2013. https://publications.lib.chalmers.se/records/fulltext/176377/176377.pdf

58. Shinde N, Aloorkar N, Kulkarni A. Recent Advances in Vesicular Drug Delivery System. *Res J Pharm Dos Forms Technol*. 2014;6(2):110-120.

59. Uchegbu IF, Vyas SP. Non-ionic surfactant based vesicles (niosomes) in drug delivery. *Int J Pharm*. 1998;172(1-2):33-70.

60. Balakrishnan P, Yong S, Shanmugam S, et al. Formulation and in vitro assessment of minoxidil niosomes for enhanced skin delivery. *Int J Pharm*. 2009;377(1-2):1-8.

61. Permegear Diffusion Testing Fundamentals. Available from https://permegear.com/wp-content/uploads/2015/08/primer.pdf. Accessed 11/09/2019

62. Van den Bergh BA et al. Interactions of elastic and rigid vesicles with human skin in vitro: electron microscopy and two-photon excitation microscopy. Biochimica et Biophysica Acta (BBA)-Biomembranes. 1999;1461(1):155-73.

63. El Zaafarany GM, Awad GAS, Holayel SM, Mortada ND. Role of edge activators and surface charge in developing ultradeformable vesicles with enhanced skin delivery. *Int J Pharm*. 2010;397(1-2):164-172.

64. Muzzalupo R, Tavano L, Lai F, Picci N. Niosomes containing hydroxyl additives as percutaneous penetration enhancers: Effect on the transdermal delivery of sulfadiazine sodium salt. *Colloids Surfaces B Biointerfaces*. 2014;123:207-212.

65. Negl LM, Garg AK, Chauhan M. Ultradeformable vesicles: Concept and execution. *Pharma Times*. 2009;41(9):11-14.

66. The Franz Cell Chamber. Available from http://bmctoday.net/vehiclesmatter/pdfs/thefranzcellchamber.pdf. Accessed 11/09/2019

67. Salamanca CH, Barrera-Ocampo A, Lasso JC, Camacho N, Yarce CJ. Franz diffusion cell approach for pre-formulation characterisation of ketoprofen semi-solid dosage forms. *Pharmaceutics*. 2018;10(3).

68. In Vitro Release Testing Methods for Semisolid Formulations Particle Sciences - Technical Brief. volume 10. Published 2009. Available from https://www.particlesciences.com/news/technical-briefs/2009/in-vitro-release-testing-methods.html accessed 23/01/2019

69. Shah V. *Guidance for Industry Nonsterile Semisolid Dosage Forms Scale-Up and Post Approval Changes: Chemistry, Manufacturing, and Controls; In Vitro Release Testing and In Vivo Bioequivalence Documentation*.; 1997. Available from https://www.fda.gov/regulatory-information/search-fda-guidance-documents/supac-ss-nonsterile-semisolid-dosage-forms-scale-and-post-approval-changes-chemistry-manufacturing. accessed 27/05/2021

70. Roberts MS, Anissimov YG. *Mathematical Models* in *Percutaneous Absorption* 4th ed. Taylor Francis Group; 2005 (pp. 37-80).

71. Jain S, Jain P, Umamaheshwari RB, Jain NK. Transfersomes - A Novel Vesicular Carrier for Enhanced Transdermal Delivery: Development, Characterization, and Performance Evaluation. *Drug Dev Ind Pharm*. 2003;29(9):1013-1026.

72. Ravalika V, Sailaja AK. Formulation and evaluation of etoricoxib niosomes by thin film hydration technique and ether injection method. *Nano Biomed Eng*. 2017;9(3):242-248.

73. Abdelkader H, Farghaly U, Moharram H. Effects of surfactant type and cholesterol level on niosomes physical properties and in vivo ocular performance using timolol maleate as a model drug. *J Pharm Investig*. 2014;44(5):329-337.

74. Joshi V, Brewster D, Colonero P. In vitro diffusion studies in transdermal research: A synthetic membrane model in place of human skin. *Drug Dev Deliv*. 2012;12(2):40-42.

75. *Strat-M Brochure*. www.millipore.com/StratmTool

76. Haq A, Dorrani M, Goodyear B, Joshi V, Michniak-Kohn B. Membrane properties for permeability testing: Skin versus synthetic membranes. *Int J Pharm*. 2018;539(1-2):58-64.

77. *Coldspring Harbour Phosphate Buffered Saline Perotocol*.; 2006.

78. Guarrasi V, Mangione MR, Sanfratello V, Martorana V, Bulone D. Quantification of underivatized fatty acids from vegetable oils by HPLC with UV detection. *J Chromatogr Sci*. 2010;48(8):663-668.

79. Sorbitan-monolaurate. Available from https://www.sciencedirect.com/topics/pharmacology-toxicology-and-pharmaceutical-science/sorbitan-monolaurate. Accessed 10/05/2021

80. Khoee S, Yaghoobian M. Niosomes: a novel approach in modern drug delivery systems. *Nanostructures Drug Deliv*. Published online 2017:207-237.

81. Bragagni M et al, Development and ex vivo evaluation of 5-aminolevulinic acid-loaded niosomal formulations for topical photodynamic therapy. *Int J Pharm*. 2015;494(1):258-263.

82. Manosroi A et al,. Transdermal absorption enhancement of papain loaded in elastic niosomes incorporated in gel for scar treatment. *Eur J Pharm Sci*. 2013;48(3):474-483.

83. Garg V, Singh H, Bhatia A, et al. Systematic Development of Transethosomal Gel System of Piroxicam: Formulation Optimization, In Vitro Evaluation, and Ex Vivo Assessment. *AAPS PharmSciTech*. 2017;18(1):58-71.

84. Zhang ZJ, Michniak-Kohn B. Flavosomes, novel deformable liposomes for the co-delivery of anti-inflammatory compounds to skin. *Int J Pharm*. 2020;585.